Coherent manipulation of collective three-level systems

Mihai Macovei,* Jörg Evers,† and Christoph H. Keitel‡
Max-Planck-Institut für Kernphysik, Saupfercheckweg 1, 69117 Heidelberg, Germany
and Theoretische Quantendynamik, Fakultät für Physik und Mathematik, Universität Freiburg, Hermann-Herder-Straβe 3, D-79104 Freiburg, Germany
(Received 12 August 2004; published 4 March 2005)

We investigate control schemes for the dynamics of a collection of dipole-interacting three-level atoms in V- or Λ- configuration. For this, we discuss the strong-field steady-state behavior of these systems under the influence of external parameters such as the relative phase between the two applied strong driving laser fields, the ratio of spontaneous decay and incoherent pumping rates, the splitting frequency between closely spaced atomic states, or a surrounding thermal bath. We show that these may act as convenient tools to sensitively control the collective dynamics of the atoms. As applications, we analyze the fluorescence and absorption properties of the atomic samples. Finally, we discuss the transient behavior to show that the presented schemes feature a rapid system evolution as required for many applications.

DOI: 10.1103/PhysRevA.71.033802 PACS number(s): 42.50.Fx, 42.50.Lc

I. INTRODUCTION

Apart from the fundamental interest in quantum optical systems, they are ideal candidates for a broad range of applications [1]. Typical requirements for possible applications are, e.g., a fast system evolution, complete population transfer between various system states of interest, and the availability of convenient external control parameters. Some of these requirements may be addressed by making use of collective effects, as initiated in a classic work by Dicke [2]. There, a sample of dipole-interacting atoms confined in a small linear region compared to the emission wavelength was discussed. Dicke showed that such a sample of N excited atoms forms a collective dipole moment, which leads to effects such as a superradiant fluorescence intensity proportional to N^2 and a quantum dynamics N times faster than for single atoms. He also discussed subradiant states of the atoms where, under special conditions, the emission of photons can be inhibited in the atomic sample. Since Dicke, the concept of collectivity has received considerable attention, demonstrating a wide range of collective phenomena [3–25]. Some of these effects have also been verified experimentally [7–9]. The collective spontaneous emission of an ensemble of densely spaced few-level atoms depends crucially on the environmental reservoir and may be influenced to some degree by coherent external electromagnetic fields (EMFs). For example, when a collection of two-level emitters is placed within a photonic band-gap material, the superradiant emission remains localized in the vicinity of the radiators, leading to a steady state with spontaneously broken symmetry in which the atomic system acquires a macroscopic polarization [10]. The presence of a small number of thermalized photons in a microcavity mode surrounding the atomic ensemble leads to an enhancement of the collective two-photon spontaneous decay rate [11]. Applying microwave pulses to the two lower levels of three-level atoms in a quasidegenerate Λ-type configuration one can switch the superradiant and subradiant processes from off to on and vice versa [12], while superfluorescence without inversion in such a coherently driven three-level system was shown to occur in Ref. [13]. The output intensity of a superradiant laser scales as N^2, while its linewidth is proportional to N^{-2}[14]. Controlled by coherent sources of light, collections of atomic few-level systems may exhibit interesting steady-state characteristics like jumps and discontinuous behaviors [15–20]. Similar effects are also possible with incoherent driving fields [21]. Thus collective atomic systems may have various advantages over single-atomic systems such as the acceleration of the atomic dynamics by a factor of N. This explains the considerable recent interest in collective phenomena, e.g., in quantum computation and quantum entanglement theories as well as in cooling processes. For instance, a technique for manipulating quantum information stored in collective states of mesoscopic ensembles is given in [22], while the decoherence of collective atomic spin states due to inhomogeneous coupling is discussed in [23]. Schemes for entangling atomic ensembles through laser manipulation were proposed in [24]. The collective cooling effects of atoms in a cavity were investigated both theoretically [25] and experimentally [9].

A recent idea to provide a convenient control parameter in quantum optics is based on the relative phase between driving laser fields [26–30]. Typically, this requires quantum interference between multiple-atomic-transition pathways which is known to give rise to many interesting applications [31,32]. In [26], the phase dependence of the resonance fluorescence spectrum in a single three-level Λ-type atom was discussed. In [27], spectral narrowing and fluorescence quenching in an atomic four-level system were reported. Light amplification without inversion may also be controlled by the relative phase [28]. The phase control was used in manipulating the spontaneous emission of single atoms in different surroundings as in photonic crystals [29]. The fea-

*Permanent address: Technical University of Moldova, Physics Department, Ştefan Cel Mare Av. 168, MD-2004 Chişinău, Moldova. Electronic address: macovei@usm.md
†Electronic address: joerg.evers@mpi-hd.mpg.de
‡Electronic address: keitel@mpi-hd.mpg.de

 ©2005 The American Physical Society

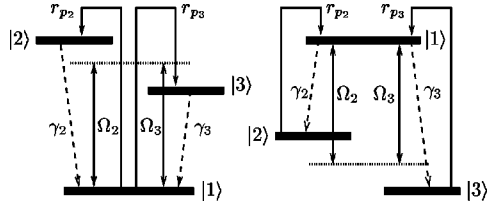

FIG. 1. Bare-state notation of the employed three-level V (left) and Λ (right) systems. Indicated also are two spontaneous decay rates γ_2 and γ_3 on the corresponding allowed transitions (dashed arrows) and the driving fields (double arrow) with the corresponding Rabi frequencies Ω_2 and Ω_3.

sibility of the control of photoabsorption via the relative phase of two fields was also demonstrated experimentally [30].

In this article, we discuss control schemes for a collection of three-level atoms embedded in a lossy cavity. Our goal is to find convenient control parameters to make the advantages of collective systems accessible for possible applications. For this we investigate the dependence of the steady-state properties of the atomic sample on external parameters such as the relative phase between two applied strong driving laser fields, the ratio of spontaneous decay and incoherent pumping rates, the splitting frequency between closely spaced atomic states, or a surrounding thermal bath. As direct applications, we also analyze the fluorescence and the absorption spectra of the systems. Finally we discuss the time evolution of the atomic sample into the steady state to verify the fast system evolution which is typical for collections of atoms. Due to the general approach, our analysis applies to atoms in both V and Λ configurations as shown in Fig. 1, and allows us to obtain analytical expressions for the steady-state solutions of the discussed setups.

By appropriately choosing the relative phase, all atoms may be trapped in the upper atomic state doublet of the three-level systems in V configuration, and in the lower doublet for the Λ system. Similar effects occur without phase-dependent terms if the ratios of the spontaneous decay and the incoherent repumping rates are varied. In these trapping states, the total collective fluorescence light is completely suppressed for the phase-dependent scheme, while for the other scheme the inhibition of the entire collective fluorescent light occurs for the Λ atoms only. For different values of the relative phase or of the ratio of spontaneous decay rates and incoherent repumping these doublet states may also be partially depleted. Increasing the number of involved atoms leads to a more rapid transfer of the atoms into the trapping state or vice versa. This property may be used to build fast optical switching devices (switching time $t_s \sim N^{-1}$) conveniently controlled by the relative phase of the two laser fields. As an additional weak probe beam would experience absorption or gain depending on the steady state of the collection of atoms, this fast switching between the ground and the excited states might be used to construct a quantum optical transistor. We further show that the system dynamics may also be controlled by surrounding thermal fields and by the splitting frequency between the two closely spaced atomic bare states in the V- and Λ-type systems.

The paper is organized as follows. In Sec. II we introduce the various systems of interest discussed in this article and derive the corresponding master equation. In Sec. III the exact steady-state solution to this master equation is derived and discussed for several system setups. The following Sec. IV analyzes the transient behavior of the atomic samples. Sections V and VI investigate the fluorescence and absorption properties of the collective systems, respectively. Finally the results are summarized in Sec. VII.

II. THE MODEL AND MASTER EQUATION

Our model system consists of an ensemble of three-level atoms with a configuration of energy levels as shown in Fig. 1. We discuss both V and Λ configurations as these may be described in a uniform manner with the employed ansatz. As we want to describe the collective effects of the system by using collective operators, we assume the sample of atoms to be confined in a region which is small as compared to the wavelengths λ of the atomic transitions (Dicke model). Furthermore we impose the condition $d\lambda^3 \sim 1$ for the atomic density d such that collisions among the radiators are avoided in our setup. However, the low density also restricts the possible number of atoms in the sample. In order to overcome this restriction, it is possible to relax the above condition that the sample is small as compared to the incident wavelength for one or two dimensions. This yields pencil-shaped or disk-shaped samples. Our analysis also applies to these geometries, if one introduces a geometry-dependent factor μ as prefactor to the atomic decay widths [4–6]. In these setups, dephasing by dipole-dipole interactions among the radiators is avoided due to the low density, but the total number of atoms and thus the collective effects can still be considerable due to the extended geometry.

The two dipole-allowed transitions between the states $|2\rangle \leftrightarrow |1\rangle$ and $|3\rangle \leftrightarrow |1\rangle$ are driven independently by two strong coherent fields with Rabi frequencies $2\Omega_2$ and $2\Omega_3$ and phases ϕ_2 and ϕ_3, respectively. In the V system, the upper states $|2\rangle$ and $|3\rangle$ decay to the ground state with decay rates $2\gamma_2$ and $2\gamma_3$, while in the Λ system, the upper state $|1\rangle$ decays to the ground states $|2\rangle$ and $|3\rangle$ with rates $2\gamma_2$ and $2\gamma_3$.

Adopting the mean-field, dipole, and rotating-wave approximations, one may write the Hamiltonian describing the interaction of the V-type atoms with the cavity EMF and the external coherent fields in the interaction picture as [15]

$$H = H_f + H_0 + H_i, \tag{1}$$

where

$$H_f = \hbar(\omega_c - \omega_L)a^\dagger a,$$

$$H_0 = \hbar\Delta_2 S_{22} + \hbar\Delta_3 S_{33} + \sum_{\alpha\in\{2,3\}} \{\hbar\Omega_\alpha S_{\alpha 1} e^{i\phi_\alpha} + \text{H.c.}\},$$

$$H_i = i \sum_{\alpha\in\{2,3\}} (\vec{g}\cdot\vec{d}_{\alpha 1})\{a^\dagger S_{1\alpha} - S_{\alpha 1} a\}.$$

Here, ω_c is the frequency of the cavity mode, and $\omega_L \equiv \omega_{L2} = \omega_{L3}$ is the frequency of the two applied external fields with

detunings $\Delta_2=\omega_{21}-\omega_L$ and $\Delta_3=\omega_{31}-\omega_L$ to the atomic transition frequencies ω_{21} and ω_{31}. $(\vec{g}\cdot\vec{d}_{\alpha 1})$ describes the atom-field coupling, and $a^\dagger$ (a) are the creation (annihilation) operators for cavity photons $(a=[a^\dagger]^\dagger)$. The collective operators

$$S_{\alpha\beta}=\sum_{j=1}^{N}S_{\alpha\beta}^{(j)}=\sum_{j=1}^{N}|\alpha\rangle_{jj}\langle\beta|\equiv|\alpha\rangle\langle\beta| \tag{2}$$

describe transitions among the collective states $|\beta\rangle$ and $|\alpha\rangle$ for $\alpha\neq\beta$ and collective populations for $\alpha=\beta$, and satisfy the commutation relation $[S_{\alpha\beta},S_{\beta'\alpha'}]=\delta_{\beta\beta'}S_{\alpha\alpha'}-\delta_{\alpha\alpha'}S_{\beta'\beta}$ for $\{\alpha,\alpha',\beta,\beta'\}\in\{1,2,3\}$.

In Eq. (1), the first term represents the free EMF, whereas the second term is the Hamiltonian describing the free atoms and the coupling to the external coherent fields. The last term considers the interaction of the atomic sample with the cavity mode.

In the Heisenberg picture and for V-type samples, the time evolution of the mean value of an arbitrary collective atomic operator $O(t)$ may be written as follows [3,11]:

$$\frac{d}{dt}\langle O(t)\rangle-\frac{i}{\hbar}\langle[H_0,O(t)]\rangle=-\sum_{\alpha\in\{2,3\}}\frac{(\vec{g}\cdot\vec{d}_{\alpha 1})}{\hbar}\{\langle a^\dagger[S_{1\alpha},O(t)]\rangle+\langle[O(t),S_{\alpha 1}]a\rangle\}, \tag{3}$$

where the notation $\langle\cdots\rangle$ indicates averaging over the initial state of both the atoms and the thermal EMF environment system. Assuming that the atomic subsystem couples weakly to the surrounding EMF, i.e., in the bad-cavity limit, the EMF operators can be eliminated from the above equation of motion. On solving formally the Heisenberg equations for the cavity field operators one can represent the solutions in the form [33]

$$a^\dagger(t)=a_f^\dagger(t)+a_s^\dagger(t), \tag{4}$$

with

$$a_f^\dagger(t)=a_f^\dagger(0)e^{i(\delta_c+ik)t}, \tag{5}$$

$$a_s^\dagger(t)=\hbar^{-1}\sum_{\alpha\in\{2,3\}}\frac{(\vec{g}\cdot\vec{d}_{\alpha 1})}{k-i(\delta_c-\Delta_\alpha)}S_{\alpha 1}(t), \tag{6}$$

as the free and the source parts of the EMF operators, respectively. Here, k is the rate at which the cavity is losing photons, and $\delta_c=\omega_c-\omega_L$. To represent the cavity field operators in this way one has to impose the restriction that the time required for a light signal to cross the atomic sample is shorter than any other relaxation times in the system, i.e., the system loses the memory of its past. Introducing Eq. (4) in Eq. (3) and using Bogoliubov's lemma [34] to represent the free atom-field correlators $\langle a_f^\dagger(t)A(t)\rangle$ and $\langle A(t)a_f(t)\rangle$ via the atomic operators and the bath characteristics only, we obtain an equation describing the quantum dynamics of any collective atomic operator:

$$\begin{aligned}\frac{d}{dt}\langle O(t)\rangle-\frac{i}{\hbar}\langle[H_0,O(t)]\rangle=&-\sum_{\alpha\in\{2,3\}}\Gamma_\alpha\{\langle S_{\alpha 1}[S_{1\alpha},O(t)]\rangle\\&+\bar{n}_\alpha\langle[S_{\alpha 1},[S_{1\alpha},O(t)]]\rangle\}\\&-\sum_{\alpha\neq\beta\in\{2,3\}}\Gamma_{\alpha\beta}\{\langle S_{\alpha 1}[S_{1\beta},O(t)]\rangle\\&+\bar{n}_\alpha\langle[S_{\alpha 1},[S_{1\beta},O(t)]]\rangle\}+\text{H.c.}\end{aligned} \tag{7}$$

Here, the decay constants are

$$\Gamma_\alpha=\frac{(\vec{g}\cdot\vec{d}_{\alpha 1})^2}{\hbar^2[k-i(\delta_c-\Delta_\alpha)]}, \tag{8}$$

$$\Gamma_{\alpha\beta}=\frac{(\vec{g}\cdot\vec{d}_{\alpha 1})(\vec{g}\cdot\vec{d}_{\beta 1})}{\hbar^2[k-i(\delta_c-\Delta_\alpha)]} \tag{9}$$

for $\alpha\neq\beta\in\{2,3\}$, and $\bar{n}_\alpha=[\exp(\xi\hbar\omega_{\alpha 1})-1]^{-1}$ is the mean thermal photon number at the atomic frequencies $\omega_{\alpha 1}=\omega_\alpha-\omega_1$ and at temperature T $[\xi=(k_BT)^{-1}$ with the Boltzmann constant $k_B]$. Note that in Eq. (7) for the in general non-Hermitian atomic operators $O(t)$, the H.c. terms should be evaluated without conjugating $O(t)$, i.e., by replacing $O^+(t)$ with $O(t)$ in the Hermitian conjugate parts. Next, from Eq. (7), one can obtain the equation for the density matrix $\rho(t)$. As

$$\mathrm{Tr}\left(\frac{d}{dt}O(t)\rho(0)\right)=\mathrm{Tr}\left(\frac{d}{dt}\rho(t)O(0)\right),$$

we obtain for a V-type sample the density matrix [35]

$$\begin{aligned}\frac{d}{dt}\rho(t)+\frac{i}{\hbar}[H_0,\rho]=&-\sum_{\alpha\in\{2,3\}}\big(\Gamma_\alpha\{[S_{\alpha 1},S_{1\alpha}\rho]\\&+\bar{n}_\alpha[S_{\alpha 1},[S_{1\alpha},\rho]]\}+r_{p\alpha}[S_{1\alpha},S_{\alpha 1}\rho]\big)\\&-\sum_{\alpha\neq\beta\in\{2,3\}}\big(\Gamma_{\alpha\beta}\{[S_{\alpha 1},S_{1\beta}\rho]\\&+\bar{n}_\alpha[S_{\alpha 1},[S_{1\beta},\rho]]\}\big)+\text{H.c.}\end{aligned} \tag{10}$$

In Eqs. (7) and (10), the first term following $d\langle O(t)\rangle/dt$ and $d\rho(t)/dt$ describes the coupling to the coherent driving fields. The second term considers the incoherent interaction of the atomic sample with the environmental bath. As expected, the thermal bath induces atomic transitions $|2\rangle\leftrightarrow|1\rangle$ and $|3\rangle\leftrightarrow|1\rangle$ with rates proportional to the mean thermal photon number at the corresponding atomic transition frequency. In Eq. (10), we additionally introduced phenomenologically an incoherent repumping of the atoms from the ground to the excited levels as shown in Fig. 1, as this will turn out to be a crucial ingredient of our control schemes. These terms are proportional to the pump rates $r_{p_\alpha}(\alpha=2,3)$. The last term of Eqs. (7) and (10) accounts for the spontaneously generated coherence (SGC) or cross-coupling effects via the exchange of virtual photons on atomic transitions $|2\rangle\rightarrow|1\rangle\rightarrow|3\rangle$ or vice versa. The notation "virtual" here refers to the fact that photons involved in these processes cannot be detected. In free space, these cross-damping effects are strongly depen-

dent on the mutual orientation of the dipole moments $\vec{d}_{21}$ and $\vec{d}_{31}$ of the two transitions. It is absent for $\vec{d}_{21} \perp \vec{d}_{31}$ and is maximal for $\vec{d}_{21} \| \vec{d}_{31}$ [1]. While the condition $\vec{d}_{21} \| \vec{d}_{31}$ is rarely met in atomic setups, it is possible to overcome this difficulty by letting the atoms interact with the EMF of a preselected cavity mode in the bad-cavity limit. With suitable cavity parameters, one may obtain SGC even for initially orthogonal dipole moments, as was shown in [36]. However, our analysis does not depend explicitly on the cavity, such that different schemes which provide nonzero values for SGC may be equally applied. Following similar steps as described above, one may also derive the corresponding master equation describing a sample of Λ-type atoms. It may be obtained from Eqs. (7) and (10) by swapping the two indices of each transition operator having α or β as one of the indices, e.g., $S_{\alpha 1} \leftrightarrow S_{1\alpha}$.

III. STEADY-STATE SOLUTIONS OF THE MASTER EQUATION

In this section we derive exact strong-field steady-state solutions to the master equation Eq. (10) for several setups of interest, where with exact we mean valid for all numbers of atoms and without further approximations other than the secular approximation. We then discuss how the collective properties of the atomic samples may be modified by means of the external parameters.

A. Phase manipulation of collective processes

In this subsection, we investigate the dependence of the collective quantum dynamics on the relative phase between the applied external coherent fields [19]. For this, we assume the two atomic transitions to be degenerate and the environmental temperature to be zero, i.e., $\bar{n}_\alpha = 0$. In the V -system, with $\delta_c = \Delta_\alpha = 0$ in Eq. (10), one obtains $\gamma_\alpha := \Gamma_\alpha = (\vec{g} \cdot \vec{d}_{\alpha 1})^2 / (\hbar^2 k)$ as the spontaneous decay rates into the cavity mode on the transitions $|\alpha\rangle \rightarrow |1\rangle$, while $\gamma_{\alpha\beta} := \Gamma_{\alpha\beta} = \eta \sqrt{\gamma_\alpha \gamma_\beta}$ are the cross-damping contributions with η as a control parameter which is unity for maximal cross-damping contributions and zero if these cross-coupling terms are absent ($\alpha \neq \beta \in \{2,3\}$). The parameter η also allows one to account for possible external perturbations such as collisions which may reduce the SGC contribution. However, as was already shown for particular decoherence sources in collective systems [37], moderate disturbances may be compensated by increasing the number of atoms or the intensities of the applied fields. In particular, while η needs to be above zero, it may be less than unity in our scheme. As we are interested in the strong-field limit $\Omega_\alpha \gg N\gamma_\alpha$, $N r_{p_\alpha} (\alpha \in \{2,3\})$, we change to the dressed-state picture (see Fig. 2):

$$|\Psi_1\rangle = \cos\tilde{\theta}|2\rangle - \sin\tilde{\theta}|3\rangle,$$

$$|\Psi_2\rangle = \frac{1}{\sqrt{2}}\{\sin\tilde{\theta}|2\rangle + \cos\tilde{\theta}|3\rangle + |1\rangle\},$$

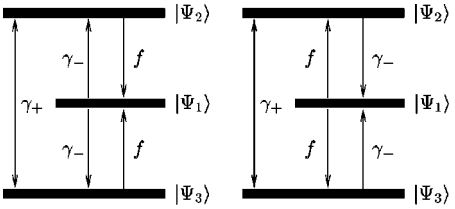

FIG. 2. Dressed-state notation of the three-level systems indicating the allowed transitions among the dressed states together with the dressed relative decay rates. The left scheme stands for the V radiators while the right one represents the Λ atoms.

$$|\Psi_3\rangle = \frac{1}{\sqrt{2}}\{-\sin\tilde{\theta}|2\rangle - \cos\tilde{\theta}|3\rangle + |1\rangle\}, \tag{11}$$

where $\sin\tilde{\theta} = \Omega_2/\tilde{\Omega}$, and $\cos\tilde{\theta} = \Omega_3/\tilde{\Omega}$ with $\tilde{\Omega} = \sqrt{\Omega_2^2 + \Omega_3^2}$. We also apply the transformation $\tilde{S}_{\alpha 1} = S_{\alpha 1} e^{i\phi_\alpha} (\tilde{S}_{1\alpha} = S_{1\alpha} e^{i\phi_\alpha})$ in Eq. (10) for V- (Λ-)type atoms and drop the tilde afterward for notational simplicity. Taking advantage of Eqs. (11) in the transformed Eq. (10) and neglecting terms that oscillate with frequencies $\tilde{\Omega}$ and larger in a secular approximation, one arrives at the following dressed master equation:

$$\begin{aligned}\dot{\rho} + i\tilde{\Omega}[R_z, \rho] = &-\frac{1}{2}\{\gamma_-([R_{12}, R_{21}\rho] + [R_{13}, R_{31}\rho]) \\ &+ f([R_{21}, R_{12}\rho] + [R_{31}, R_{13}\rho])\} \\ &- \frac{\gamma_+}{4}\{[R_{23}, R_{32}\rho] + [R_{32}, R_{23}\rho] + [R_z, R_z\rho]\} \\ &+ \text{H.c.},\end{aligned} \tag{12}$$

where

$$\gamma_- = \gamma_2 \cos^2\tilde{\theta} + \gamma_3 \sin^2\tilde{\theta} - \gamma_{23} \cos(\Delta\phi) \sin 2\tilde{\theta}, \tag{13}$$

$$f = r_{p_2} \cos^2\tilde{\theta} + r_{p_3} \sin^2\tilde{\theta}, \tag{14}$$

$$\begin{aligned}\gamma_+ = &(\gamma_2 + r_{p_2}) \sin^2\tilde{\theta} + (\gamma_3 + r_{p_3}) \cos^2\tilde{\theta} \\ &+ \gamma_{23} \cos(\Delta\phi) \sin 2\tilde{\theta}.\end{aligned} \tag{15}$$

Here, $R_z = R_{22} - R_{33}$ with $R_{\alpha\beta} = |\Psi_\alpha\rangle\langle\Psi_\beta|$ for $\{\alpha, \beta\} \in \{1,2,3\}$ and $\Delta\phi := \phi_2 - \phi_3$. The operators $R_{\alpha\beta}$ represent a rotation of the collective bare-state operators and hence satisfy the same commutation relation as the old operators. As with the bare-state equations, the corresponding dressed master equation for a Λ system is the same as Eq. (12) except for the permutation of the indices in the right-hand part of it. γ_- can be interpreted as a dressed decay rate, f is a dressed pumping rate, and γ_+ describes the distribution of population between two of the dressed states as indicated in Fig. 2.

The dressed master equations for both V- and Λ-type samples admit an exact steady-state solution (subindex s) of the following form:

TABLE I. Mean steady-state values of the collective operators.

	$X=0$	$X=1$	$X\to\infty$
$\langle R\rangle_s$	0	$2/3N$	N
$\langle R^2\rangle_s$	0	$1/2N(N+1/3)$	N^2
$\langle R_{11}\rangle_s$	N	$1/3N$	0

$$\rho_s = Z^{-1}\sum_{r=0}^{N} X_{V(\Lambda)}^{r}\sum_{m=0}^{r}|r,m\rangle\langle m,r|. \tag{16}$$

Here, $|r,m\rangle$ are eigenstates of the operators $R=R_{22}+R_{33}$, R_{33} and $R_{11}+R_{22}+R_{33}$ with eigenvalues r,m, and N, respectively, and Z is a normalization constant chosen such that $\mathrm{Tr}\{\rho_s\}=1$ [17,19,20,35]. The coefficient X_V is given by the ratio of the dressed spontaneous decay rate γ_- to the dressed pumping rate f, and X_Λ is the inverse of X_V (see Fig. 2):

$$X_V = \frac{\gamma_-}{f}, \quad X_\Lambda = \frac{f}{\gamma_-}. \tag{17}$$

The steady-state atomic population of the dressed states is then given by

$$\langle R_{11}\rangle_s = \frac{NX^{N+2} - (N+2)X^{N+1} + N(X-1) + 2X}{(X-1)[(N+1)X^{N+2} - (N+2)X^{N+1} + 1]}$$

and $\langle R_{33}\rangle_s = \langle R_{22}\rangle_s = \langle R\rangle_s/2$ with $\langle R\rangle_s = N - \langle R_{11}\rangle_s$. Here, we have dropped the index of X because all discussed populations depend identically on the respective X_V and X_Λ parameters for both systems. The steady-state behavior of the collective atomic operators for some particular values of the parameter X is given in Table I. The mean steady-state atomic population in the collective bare state $|1\rangle$ can be calculated by the relation $\langle S_{11}\rangle_s = [N - \langle R_{11}\rangle_s]/2$.

For simplicity, in the following we consider the case $\gamma_2 = \gamma_3 =: \gamma_0$, $r_{p_2} = r_{p_3} =: r_p$. The parameter X may then be written as $X_V = \mathcal{C}\{1 - \eta \sin 2\tilde{\theta}\cos\Delta\phi\}$ with $X_\Lambda = X_V^{-1}$. $\mathcal{C} = \gamma_0/r_p$ is the ratio of spontaneous decay and incoherent repumping in the atomic systems. Both $\mathcal{C}$ and X_V (X_Λ) will turn out to crucially influence the system behavior.

First we investigate the case $\eta=1$, $\tilde{\theta}=\pi/4$, and $\mathcal{C}=4$, i.e., the decay dominates over the repumping. Figure 3(a) shows the steady-state population per atom in the collective dressed state $|\Psi_1\rangle$ for different numbers of atoms N against the relative phase between the two applied strong laser fields for V-type systems. The corresponding results for the Λ system are displayed in Fig. 4(a). As can be seen, a single V-type atom ($N=1$) may only be trapped in $|\Psi_1\rangle$ for $\Delta\phi = n \times 2\pi$ ($n \in \{0,1,\ldots\}$), while a single Λ-type atom may not be trapped with incoherent pumping. However, a collection of atoms ($N \gg 1$) allows for trapping for both the V and the Λ systems. The range $\delta(\Delta\phi)$ of the phase difference, for which the collective coherent population trapping effect occurs, grows with an increasing number of atoms, until in the limit $N\to\infty$ the system exhibits jumps between two states with either all or none of the population in the collective state

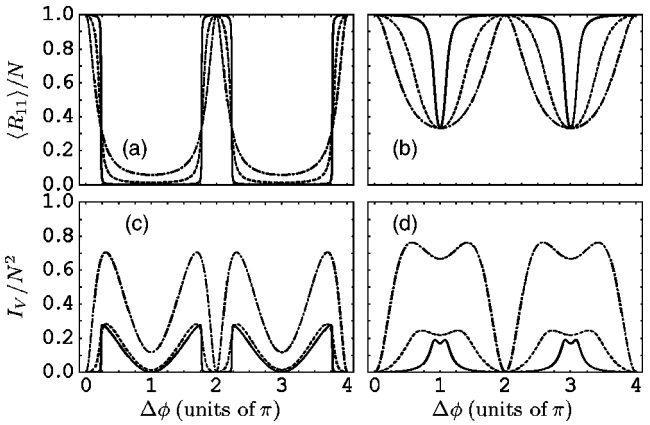

FIG. 3. The dependence of (a), (b) the steady-state population of the collective dressed state $|\Psi_1\rangle$ and (c), (d) of the total collective steady-state fluorescence intensity as a function of the relative phase $\Delta\phi$ for the V system. The dash-dotted, dashed, and solid curves correspond to $N=1$, 10, and 200, respectively. Further $\tilde{\theta} = \pi/4$, $\eta=1$, $\Phi(r)=1$, and $\mathcal{C}=(a)$, (c) 4, (b), (d) 0.5.

$|\Psi_1\rangle$. In order to understand this behavior of the dressed-state steady-state population $|\Psi_1\rangle$, we take the limit $N\to\infty$ of its population per atom $\langle R_{11}\rangle_s/N$. As shown in Table I, one obtains 1 for $0 \leqslant X < 1$, 1/3 for $X=1$, and 0 for $X>1$. Thus the jumps occur at $X=1$, which in our example $\eta=1$, $\tilde{\theta}=\pi/4$, and for $\mathcal{C}>0.5$, corresponds to a phase difference of $\cos\Delta\phi = 1 - 1/\mathcal{C}$. Then the trapping ranges for the V and Λ systems are given by

$$\delta(\Delta\phi)_V = 2\arccos[1 - 1/\mathcal{C}], \tag{18}$$

$$\delta(\Delta\phi)_\Lambda = 2(\pi - \arccos[1 - 1/\mathcal{C}]). \tag{19}$$

On increasing $\mathcal{C}$ by decreasing the incoherent pump rates, the trapping ranges of the V system become very narrow while for the Λ radiators the trapping domains become wider. Note that in the absence of incoherent pumping ($\mathcal{C}\to\infty$) only the Λ-type samples can be trapped, including the single-atom case $N=1$. In this case without incoherent pumping, the steady-state populations of the dressed states of both samples are insensitive to the relative phase $\Delta\phi$, except for the spe-

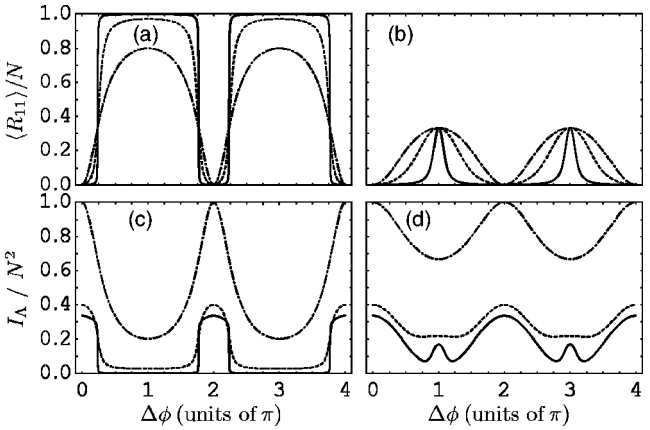

FIG. 4. The same as in Fig. 3 but for the Λ sample.

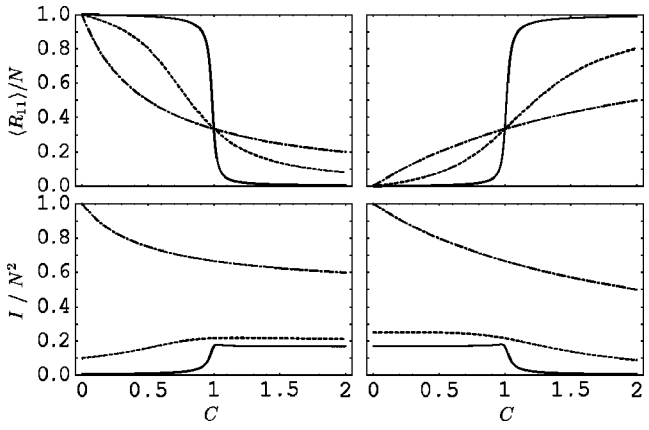

FIG. 5. The dependence of the steady-state population in the collective dressed state $|\Psi_1\rangle$ and the total collective intensity on the ratio $\mathcal{C}=\gamma_0/r_p$. The left column corresponds to the V sample, the right to the Λ system. The dash-dotted, dashed, and solid curves correspond to $N=1$, 10, and 200, respectively. Here, $\eta=0$, $\tilde{\theta}=\pi/4$, and $\Phi(r)=1$.

cial case $\Delta\phi=2\pi n$ and $\tilde{\theta}=\pi/4$, where the collective dressed state $|\Psi_1\rangle$ decouples from the interaction with the environmental bath.

For $\mathcal{C}\leqslant 0.5$, i.e., dominating repumping, the results shown in Figs. 3(b) and 4(b) may be interpreted accordingly. The main difference is that the condition $X_V\leqslant 1(X_\Lambda\geqslant 1)$ is always satisfied, such that the collective dressed state $|\Psi_1\rangle$ is never entirely depleted in the V system and never fully populated in the Λ case. Thus no discontinuities can be observed.

Figures 5 and 6 (upper row) show the dependence of the steady-state population in the collective dressed state $|\Psi_1\rangle$ on the parameter $\mathcal{C}$, for both $\eta=0$ and $\eta=1$. In these cases the trapping is feasible for a large sample of V- or Λ-type atoms and the collective jumps (or discontinuities for $N\to\infty$) occur at $X=1$. These discontinuities may be explained as phase transitions [17] and are due to the fact that the sample of atoms forms a collective dipole moment which evolves on a time scale N times faster than the single-atom dipole moment, thus allowing for corresponding changes of the collective dressed steady-state populations. They occur for the $V(\Lambda)$ system at the points where the dressed spontaneous

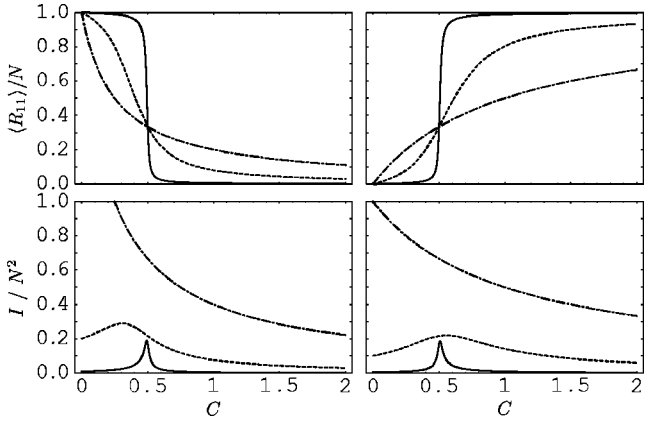

FIG. 6. The same as in Fig. 5 but for $\eta=1$ and $\Delta\phi=\pi$.

decay out of (into) state $|\Psi_1\rangle$ just equals the dressed pumping in the reverse direction (see Fig. 2).

We end this subsection by noting that in the strong-field limit with incoherent repumping the trapping of a large ensemble in principle does not require the presence of the cross-damping terms, that is, for large samples one can trap the radiators with both $\eta=0$ and $\eta\neq 0$. Also, for large systems, the collective trapping dressed state $|\Psi_1\rangle$ can be completely depopulated in both cases. However, for smaller V-type samples it is difficult to trap the atoms without cross-coupling terms since then one needs $\mathcal{C}=0$, i.e., $r_p\to\infty$ or $\gamma_0\to 0$. Similarly, trapping of a small sample of Λ atoms without the cross-damping terms requires $\mathcal{C}\to\infty$, i.e., $r_p\to 0$ or $\gamma_0\to\infty$. However, this limiting case corresponds to the well-known decay-independent coherent population transfer mechanism between states $|2\rangle$ and $|3\rangle$ via adapting the intensities of the driving fields appropriately. Thus the cross-damping terms make the presented schemes more efficient especially for smaller samples. Furthermore, without the cross-damping terms, no phase control of the system dynamics is possible.

B. Magnetic and thermal influences on collective processes

In this section we investigate the influence of the thermal environment and the splitting frequency between the two closely spaced atomic states on the collective quantum dynamics for both the V and the Λ systems [20]. The influence of incoherent driving fields on the collective dynamics is discussed in [21]. We assume the frequencies of the two coherent driving fields to be equal to the average of the two atomic transition frequencies, $\omega_0:=(\omega_{21}+\omega_{31})/2$, such that $\Delta:=\Delta_2=-\Delta_3$. Also, we choose equal phases $\phi_2=\phi_3=0$, no incoherent pumping $r_p=0$, and cavity parameters $\delta_c=0$ and $k\gg\Delta$. The corresponding master equation may then be obtained from Eq. (10). In the following, we again discuss the strong-field limit $\Omega_\alpha\gg N\gamma_\alpha(\bar{n}+1)$, $\alpha\in\{2,3\}$, and consider two different cases for the splitting between the two closely spaced upper (lower) atomic states in the V- (Λ-)type system. The first configuration is given by $\Omega_0:=\Omega_2=\Omega_3$ and will be referred to as the *nondegenerate system*. The second configuration may be obtained by assuming $\omega_{23}=0$ and will be referred to as the *degenerate* system.

For the nondegenerate emitters we transfer into the following dressed-state picture:

$$|\Psi_2\rangle=\frac{1}{2}\{(\sin\theta+1)|2\rangle-(\sin\theta-1)|3\rangle\}+\frac{1}{\sqrt{2}}\cos\theta|1\rangle,$$

$$|\Psi_1\rangle=\frac{1}{\sqrt{2}}\cos\theta\{|2\rangle-|3\rangle\}-\sin\theta|1\rangle,$$

$$|\Psi_3\rangle=\frac{1}{2}\{(\sin\theta-1)|2\rangle-(\sin\theta+1)|3\rangle\}+\frac{1}{\sqrt{2}}\cos\theta|1\rangle \tag{20}$$

with $\sin\theta=\omega_{23}/(2\Omega)$, $\cos\theta=\sqrt{2}\Omega_0/\Omega$, and $\Omega=\sqrt{2\Omega_0^2+(\omega_{23}/2)^2}$. For the degenerate systems we use the

transformation in Eq. (11). Note that throughout the article the expressions containing the generalized Rabi frequency with tilde (i.e., $\tilde{\Omega}$) refer to the degenerate atomic ensembles, while those without the tilde (i.e., Ω) belong to the nondegenerate atomic samples. Substituting Eqs. (11) and (20) in Eq. (10) and neglecting terms that oscillate with frequencies $\Omega(\tilde{\Omega})$ and larger in a secular approximation as well as assuming that $\gamma_0 := \gamma_2 = \gamma_3 = \gamma_{23}$ (i.e., $\eta = 1$), one can show that the dressed master equation has the same form as Eq. (12), but with

$$\gamma_- = 2\gamma_0 \bar{n} \sin^2 \theta, \tag{21}$$

$$f = 2\gamma_0 (1 + \bar{n}) \sin^2 \theta, \tag{22}$$

$$\gamma_+ = 2\gamma_0 (1 + 2\bar{n}) \cos^2 \theta \tag{23}$$

for the nondegenerate system, and

$$\gamma_- = \gamma_0 (1 + \bar{n})(1 - \sin 2\tilde{\theta}), \tag{24}$$

$$f = \gamma_0 \bar{n} (1 - \sin 2\tilde{\theta}), \tag{25}$$

$$\gamma_+ = \gamma_0 (1 + 2\bar{n})(1 + \sin 2\tilde{\theta}) \tag{26}$$

for the degenerate system. Here, $\bar{n} = [\exp(\xi \hbar \omega_0) - 1]^{-1}$ is the mean thermal photon number at the average atomic frequency ω_0 and at temperature T. Thus, the exact steady-state solution of the dressed master equation is again given by Eq. (16), but with coefficients $X_{V(\Lambda)}$ given by

$$X_V = \frac{\bar{n}}{\bar{n} + 1}, \quad X_\Lambda = \frac{\bar{n} + 1}{\bar{n}} \text{ for } \Omega_2 = \Omega_3, \quad \omega_{23} \neq 0,$$

$$X_V = \frac{\bar{n} + 1}{\bar{n}}, \quad X_\Lambda = \frac{\bar{n}}{\bar{n} + 1} \text{ for } \Omega_2 \neq \Omega_3, \quad \omega_{23} = 0.$$

The dressed steady-state atomic populations then can be evaluated using Eq. (16). On inserting the above coefficients $X_{V(\Lambda)}$ into Eq. (16) we obtain that the collective dressed-state population of the degenerate V-type system is equal to the corresponding population of the nondegenerate Λ-type atoms. Correspondingly, nondegenerate V and degenerate Λ systems are equivalent (see Fig. 7). For a small mean number $\bar{n}$ of thermal photons and a large sample, i.e., $N \gg 1$, all the steady-state atomic population is in the collective dressed state $|\Psi_1\rangle$ for the V scheme with nondegenerate upper bare states as well as for the Λ atoms with degenerate lower bare atomic states. In contrast to that, the collective dressed state $|\Psi_1\rangle$ will be empty for Λ atoms with nondegenerate lower bare atomic states and for V atoms with degenerate upper bare states in this case (see Fig. 7). For an intense thermal bath, $\bar{n} \gg 1$ such that $X \approx 1$, all the collective dressed states are populated equally, i.e., $\langle R_{11} \rangle_s = \langle R_{22} \rangle_s = \langle R_{33} \rangle_s = N/3$. These observations may be explained by noting that for $\omega_{23} \neq 0$ (nondegenerate case) the spontaneous emission populates the collective dressed state $|\Psi_1\rangle$ for the V emitters and depopulates it for the Λ atoms, while for the degenerate case $\omega_{23} = 0$ (and $\tilde{\theta} \neq \pi/4$) the spontaneous emission acts in the opposite direction, i.e., depopulates the $|\Psi_1\rangle$ dressed state for V atoms and populates it for Λ radiators. In the special case $\tilde{\theta} = \pi/4$ and $\omega_{23} = 0$, the collective dressed state $|\Psi_1\rangle$ decouples from the interaction with the environment such that the steady-state behavior in this case depends on the initial preparation of the sample.

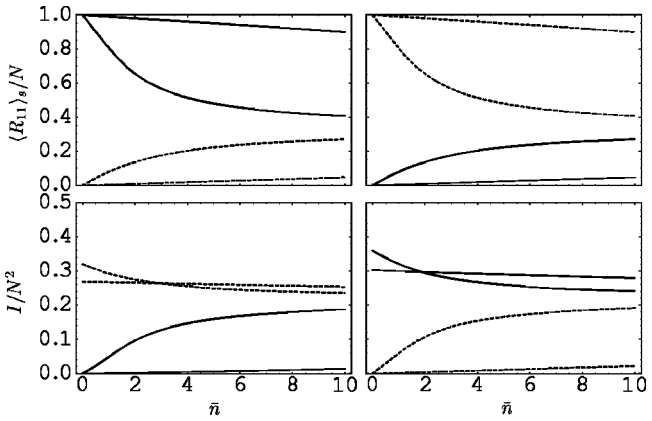

FIG. 7. The dependence of the collective steady-state population of dressed state $|\Psi_1\rangle$ and the total fluorescence intensity on both transitions versus the mean thermal photon number $\bar{n}$. The left column corresponds to V systems, the right to Λ-type systems. Dashed lines represent degenerate schemes, while the solid curves are for the nondegenerate closely spaced bare-state models. Here, $N = 200$ (outer curves) and 10 (inner curves).

Thus, by slightly varying the frequency difference ω_{23}, e.g., via an external applied magnetic field, in addition to changing the intensities of the external coherent sources, the dressed spontaneous decay reverses its direction which results in large changes of the collective atomic population of the trapping state $|\Psi_1\rangle$. In Fig. 7, these changes correspond to jumps from the upper branch to the lower one or vice versa.

In conclusion, the strongly driven atomic three-level samples allow for a substantial modification of the steady-state population distribution controlled by various external parameters. The third atomic level together with the specific choices of external influences discussed in this section thus allows for a better control over the collective system dynamics than in corresponding two-level schemes [15], where, for example, steady-state population inversion requires the presence of special environments such as photonic crystals [37]. Particular examples for this are the phase control and the strong dependence of the results on the splitting frequency between the two upper (lower) states in the V- (Λ-)type sample.

IV. TIME EVOLUTION OF THE DRESSED-STATE POPULATIONS

While up to now we have focused our analysis on the steady-state properties of the given system, in this section we discuss the transient system dynamics. This is of particular interest for possible applications, which usually rely on a fast evolution into the various stable configurations. From the

master equation Eq. (12) for the collective population in the dressed state $|\Psi_1\rangle$ of a degenerate V sample we obtain:

$$\frac{d}{dt}\langle R_{11}(t)\rangle_V = -\gamma_-\{\langle R_{12}R_{21}\rangle + \langle R_{13}R_{31}\rangle\} + f\{\langle R_{21}R_{12}\rangle + \langle R_{31}R_{13}\rangle\}. \quad (27)$$

For a Λ sample the corresponding equation may be obtained from Eq. (27) by exchanging $\gamma_- \leftrightarrow f$. Generally, for a collection of atoms it is difficult to obtain a closed system of equations for the atomic population operators, because the equations for the first-order atomic correlators are expressed in terms of the second-order ones, the equations for second-order atomic correlators are represented via the third-order correlators, and so on. However, we can solve Eq. (27) approximately by neglecting the fluctuation of the mean population in state $|\Psi_1\rangle$ if the number of atoms N is large. Thus for $N \gg 1$, the collective second-order atomic correlators my be decoupled as follows [38]:

$$\langle R_{\alpha\beta}R_{\beta\alpha}\rangle \approx \langle R_{\alpha\alpha}\rangle\langle 1 + R_{\beta\beta}\rangle \quad (28)$$

for $\beta \neq \alpha$. In this approximation, for V and Λ samples, the time-dependent dressed population of $|\Psi_1\rangle$ is given by

$$\langle R_{11}(t)\rangle = \frac{a - b\dfrac{a-R_0}{b-R_0}e^{-|\gamma(a-b)t|}}{1 - \dfrac{a-R_0}{b-R_0}e^{-|\gamma(a-b)t|}}, \quad (29)$$

with initial condition $R_0 = \langle R_{11}(0)\rangle$, $\gamma = (\gamma_- - f)$, and $X \neq 1$. If $X > 1$, then in the limit $N \to \infty$ one has $a \to 0$, $b \to N$, while for $X < 1$, one obtains $a \to N$ and $b \to 0$. For $X = 1$, the exact solution which is valid for any number of atoms is

$$\langle R_{11}(t)\rangle = \frac{N}{3} + \left\{\langle R_{11}(0)\rangle - \frac{N}{3}\right\}e^{-3\gamma_e t}. \quad (30)$$

For $X = 1$, the above decoupling scheme is not required, as this value corresponds to the case $\gamma_- = f \equiv \gamma_e$ where Eq. (27) contains correlation functions which may be evaluated without further approximations. These results also explain the delay of the temporal evolution due to SGC effects reported in [39]. There, no incoherent pumping was considered, i.e., $f = 0$. The temporal evolution then depends on γ_-, which is a function of the relative phase $\Delta\phi$. This can result in a slowdown of the temporal evolution, as the trapping state $|\Psi_1\rangle$ decouples for $\gamma_- \to 0$. However, incoherent pumping and thus nonvanishing f allows as to avoid such problems. The time evolution of the collective populations in the remaining dressed states may be obtained from Eqs. (29) and (30) by using $\Sigma_{i=1}^{3}\langle R_{ii}(t)\rangle = N$ and $\langle R_{22}(t)\rangle = \langle R_{33}(t)\rangle$ (see Fig. 2).

Without incoherent pumping, the population in $|\Psi_1\rangle$ is again given by Eq. (29), but with $\gamma := 2\gamma_0 \sin^2\theta$ for the nondegenerate system, and $\gamma := \gamma_0(1 - \sin 2\tilde{\theta})$ the degenerate system. In the limit $N \gg \{1, \bar{n}\}$, we obtain $a \to N$ and $b \to 0$ ($a \to 0$ and $b \to N$) for the nondegenerate V(Λ) ensembles or vice versa for degenerate configurations. Here, one has to exclude the special cases $\theta = 0$ and $\tilde{\theta} = \pi/4$, as then the trapping state $|\Psi_1\rangle$ decouples from the interactions [39].

Thus, in summary, the time required to evolve into the steady state for $X \neq 1$ is proportional to N^{-1}, as is well known for collective systems [2–6]. This allows one to apply our scheme, e.g., to build fast optical switching devices [19].

V. THE COLLECTIVE RESONANCE FLUORESCENCE SPECTRA

To further discuss the system properties we now investigate the total steady-state spectrum $S(\omega)$ of the collective fluorescence light emitted on both transitions $|2\rangle \leftrightarrow |1\rangle$ and $|3\rangle \leftrightarrow |1\rangle$. It is given by the real part of the Fourier transform of the correlation function of the EMF [1]

$$S(\omega) \propto \lim_{t\to\infty}\int_0^t d\tau\, e^{i\omega\tau}\langle E^{(-)}(\vec{r}, t+\tau)E^{(+)}(\vec{r}, t)\rangle.$$

Here, $E^{(-)}$ and $E^{(+)}$ are the positive and negative frequency parts of the amplitude of the EMF operator E. As the radiators are embedded in the cavity, they emit photons in the cavity mode only. This means that the photons can be detected after they leak through the cavity walls. For a V-type atomic sample, in the far-zone limit, $r = |\vec{r}| \gg \lambda$, one can express the entire fluorescence spectrum via the collective atomic operators as

$$S(\omega)_V = \Phi(r)\mathrm{Re}\int_0^\infty d\tau\, e^{i(\omega-\omega_0)\tau}\{\langle S_{31}(\tau)S_{13}\rangle + \langle S_{21}(\tau)S_{12}\rangle + \eta[\langle S_{21}(\tau)S_{13}\rangle e^{-i\Delta\phi} + \langle S_{31}(\tau)S_{12}\rangle e^{i\Delta\phi}]\}, \quad (31)$$

where $\Phi(r)$ is a geometrical factor which we set equal to unity in the following. For a Λ-type system the expression for the fluorescence spectrum $S(\omega)_\Lambda$ is obtained by a permutation of the indices in the above expression, e.g., $S_{12} \leftrightarrow S_{21}$. As can be seen from the last addend in Eq. (31), for $\eta \neq 0$, in both types of samples the emission on the atomic transitions $|2\rangle \leftrightarrow |1\rangle$ and $|3\rangle \leftrightarrow |1\rangle$ is coupled. This gives rise to various spectral features which we discuss in the next section.

A. Phase manipulation of the collective spectral features

First we investigate the feasibility of phase controlling the collective resonance fluorescence spectrum emitted by a collection of degenerate V- and Λ-type radiators. Employing Eq. (11) in Eq. (31), in the secular approximation, one can represent the total fluorescence spectrum for a V-type sample in terms of the dressed atomic correlators:

$$S(\omega)_V = \mathrm{Re}\int_0^\infty d\tau\, e^{i(\omega-\omega_0)\tau}\left(\frac{\Omega_-^2}{2\tilde{\Omega}^2}\{\langle R_{12}(\tau)R_{21}\rangle + \langle R_{13}(\tau)R_{31}\rangle\} + \frac{\Omega_+^2}{4\tilde{\Omega}^2}\{\langle R_{23}(\tau)R_{32}\rangle + \langle R_{32}(\tau)R_{23}\rangle + \langle R_z(\tau)R_z\rangle\}\right), \quad (32)$$

where $\Omega_\pm^2 = \tilde{\Omega}^2\{1 \pm \eta\cos(\Delta\phi)\sin 2\tilde{\theta}\}$. On analyzing Eq. (32), we find that for $\eta = 1$ and a suitable choice of the relative phases and the intensities of the external fields, one can in-

hibit the spectral lines with intensities proportional to Ω_+ or Ω_-, respectively.

The dressed atomic correlation functions, which enter in Eq. (32), can be calculated by using Eq. (12) and the quantum regression theorem [40]. Thus, for both V- and Λ-type atoms one finds

$$\frac{d}{d\tau}\langle R_{12}(\tau)R_{21}\rangle = -i\tilde{\Omega}\langle R_{12}(\tau)R_{21}\rangle - \gamma_{V(\Lambda)}\langle R_{12}(\tau)R_{21}\rangle \mp \frac{\gamma_c}{2}\langle [N - 2R_{11}(\tau), R_{12}(\tau)]_+ R_{21}\rangle,$$

$$\frac{d}{d\tau}\langle R_{13}(\tau)R_{31}\rangle = i\tilde{\Omega}\langle R_{13}(\tau)R_{31}\rangle - \gamma_{V(\Lambda)}\langle R_{13}(\tau)R_{31}\rangle \mp \frac{\gamma_c}{2}\langle [N - 2R_{11}(\tau), R_{13}(\tau)]_+ R_{31}\rangle,$$

$$\frac{d}{d\tau}\langle R_{23}(\tau)R_{32}\rangle = 2i\tilde{\Omega}\langle R_{23}(\tau)R_{32}\rangle - \tilde{\gamma}_{V(\Lambda)} \times \langle R_{23}(\tau)R_{32}\rangle \pm \gamma_c\langle [R_{11}(\tau), R_{23}(\tau)]_+ R_{32}\rangle,$$

$$\frac{d}{d\tau}\langle R_z(\tau)R_z\rangle = -\overline{\gamma}_{V(\Lambda)}\langle R_z(\tau)R_z\rangle \pm \gamma_c\langle [R_{11}(\tau), R_z(\tau)]_+ R_z\rangle. \tag{33}$$

Here, the single-atom spectral widths of the spectral components emitted at frequencies $\omega_0 \pm \tilde{\Omega}$, $\omega_0 \pm 2\tilde{\Omega}$, and ω_0 are

$$\gamma_V = (\gamma_+ + 2\gamma_- + f)/2, \tag{34}$$

$$\tilde{\gamma}_V = (3\gamma_+ + 2f)/2, \tag{35}$$

$$\overline{\gamma}_V = \gamma_+ + f \tag{36}$$

for a V-type system, and

$$\gamma_\Lambda = (\gamma_+ + \gamma_- + 2f)/2, \tag{37}$$

$$\tilde{\gamma}_\Lambda = (3\gamma_+ + 2\gamma_-)/2, \tag{38}$$

$$\overline{\gamma}_\Lambda = \gamma_+ + \gamma_- \tag{39}$$

for a Λ-type system. Also, $\gamma_c = (\gamma_- - f)/2$, and the notation $[\cdots,\cdots]_+$ indicates the anticommutator. The last term in each equation of Eq. (33) vanishes for $N=1$. Thus, these terms proportional to the anticommutators represent the collective contribution to the spectral widths. These contributions make it difficult to find an exact solution to Eq. (33) for $N>1$. An approximate method to find the time-dependent solutions is to decouple the collective atomic correlators as in Sec. IV. For this, we represent the terms which are proportional to the anticommutator as

$$\langle [N - 2R_{11}(\tau), R_{1\alpha}(\tau)]_+ R_{\alpha 1}\rangle \approx 2\langle N - 2R_{11}\rangle_s \langle R_{1\alpha}(\tau)R_{\alpha 1}\rangle \tag{40}$$

for $\alpha \in \{2,3\}$. This procedure is valid for large atomic ensembles, i.e., $N \gg 1$, as then the fluctuations of the population in the dressed state $|\Psi_1\rangle$ are negligible. In other words, the steady-state variance $\langle \Delta R_{11}\rangle_s = [\langle R_{11}^2\rangle_s - \langle R_{11}\rangle_s^2]/N^2$ should be very small (or zero) to allow for the decoupling. It is not difficult to show that for $X>1$ and $X<1$ the steady-state variance $\langle \Delta R_{11}\rangle_s$ is zero, while for $X=1$ it is proportional to $N^{-1/2}$, i.e., $\sqrt{\langle \Delta R_{11}\rangle_s} \propto N^{-1/2}$ (see Table I). Thus, for $N \gg 1$ one introduces an error proportional to $N^{-1/2}$ in the calculations of the collective correlations functions $\langle R_{\alpha\beta}(\tau)R_{\beta\alpha}\rangle$ [38] in making use of the above decoupling scheme. After the decoupling of the collective dressed atomic correlators, one obtains the following expression for the collective resonance fluorescence spectrum:

$$S(\omega)_i = I_{\pm\tilde{\Omega}}^{(i)}\left[\frac{\Gamma_i}{\Gamma_i^2 + (\Delta - \tilde{\Omega})^2} + \frac{\Gamma_i}{\Gamma_i^2 + (\Delta + \tilde{\Omega})^2}\right] + I_{0,\pm 2\tilde{\Omega}}^{(i)} \times \left[\frac{\tilde{\Gamma}_i}{\tilde{\Gamma}_i^2 + (\Delta - 2\tilde{\Omega})^2} + 2\frac{\overline{\Gamma}_i}{\overline{\Gamma}_i^2 + \Delta^2} + \frac{\tilde{\Gamma}_i}{\tilde{\Gamma}_i^2 + (\Delta + 2\tilde{\Omega})^2}\right]. \tag{41}$$

Here, $i \in \{V, \Lambda\}$, $\Delta = \omega - \omega_0$, and we have used the equalities

$$\langle R_{12}R_{21}\rangle_s = \langle R_{13}R_{31}\rangle_s = N[\langle R\rangle_s/2 + 1] - \langle R^2\rangle_s/2 - \langle R\rangle_s, \tag{42}$$

$$\langle R_{21}R_{12}\rangle_s = \langle R_{31}R_{13}\rangle_s = (N+1)\langle R\rangle_s/2 - \langle R^2\rangle_s/2, \tag{43}$$

$$\langle R_{23}R_{32}\rangle_s = \langle R_{32}R_{23}\rangle_s = \langle R^2\rangle_s/6 + \langle R\rangle_s/3, \tag{44}$$

$$\langle R_z^2\rangle_s = 2\langle R_{23}R_{32}\rangle_s = 2\langle R_{32}R_{23}\rangle_s, \tag{45}$$

with

$$\langle R^2\rangle_s = [N^2(N+1)X^{N+4} - N(3N^2 + 6N - 1)X^{N+3} + (N+2)(3N^2 + 3N - 2)X^{N+2} + 2X + 4X^2 - (N+2)(N+1)^2X^{N+1}]/[(X-1)^2 \times \{(N+1)X^{N+2} - (N+2)X^{N+1} + 1\}]. \tag{46}$$

For both V- and Λ-type samples, the collective resonance fluorescence spectrum in general consists of five lines with

$$\Gamma_{V(\Lambda)} = \gamma_{V(\Lambda)} \pm \gamma_c[N - 2\langle R_{11}\rangle_s],$$

$$\tilde{\Gamma}_{V(\Lambda)} = \tilde{\gamma}_{V(\Lambda)} \mp 2\gamma_c\langle R_{11}\rangle_s,$$

$$\overline{\Gamma}_{V(\Lambda)} = \overline{\gamma}_{V(\Lambda)} \mp 2\gamma_c\langle R_{11}\rangle_s, \tag{47}$$

as the collective spectral widths of the spectral components emitted at frequencies $\{\omega_0 \pm \tilde{\Omega}, \omega_0 \pm 2\tilde{\Omega}, \omega_0\}$. The respective peak intensities are

$$I_{\pm\tilde{\Omega}}^{(V)} = \frac{\Omega_-^2}{2\tilde{\Omega}^2}\langle R_{12}R_{21}\rangle_s, \tag{48}$$

$$I_{0,\pm 2\tilde{\Omega}}^{(V)} = \frac{\Omega_+^2}{4\tilde{\Omega}^2}\langle R_{23}R_{32}\rangle_s, \tag{49}$$

$$I_{\pm\tilde{\Omega}}^{(\Lambda)} = \frac{\Omega_-^2}{2\tilde{\Omega}^2}\langle R_{21}R_{12}\rangle_s, \tag{50}$$

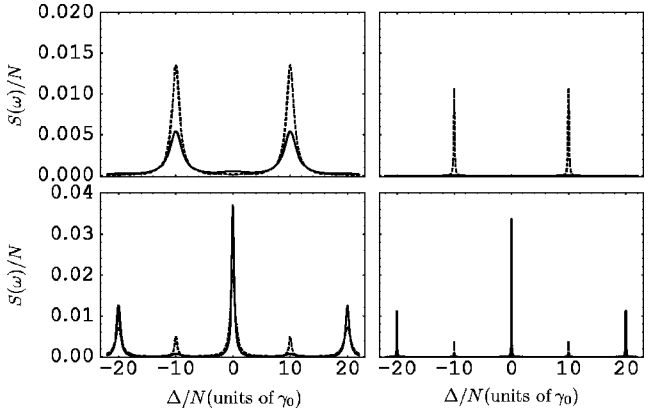

FIG. 8. Steady-state fluorescence spectra for V-type atoms. The left column corresponds to $N=10$, the right to $N=100$. The upper row displays the case $\mathcal{C}=0.5$, the lower is for $\mathcal{C}=4$. The solid lines show $\Delta\phi=\pi/2$, the dashed lines are drawn for $X=1$, i.e., $\Delta\phi=\pi(\Delta\phi=\cos^{-1}3/4)$ for $\mathcal{C}=0.5(\mathcal{C}=4)$. The other parameters are $\tilde{\Omega}=10N\gamma_0$, $\eta=1$, $\tilde{\theta}=\pi/4$, $\Phi(r)=1$.

$$I^{(\Lambda)}_{0,\pm 2\tilde{\Omega}}=\frac{\Omega_+^2}{4\tilde{\Omega}^2}\langle R_{32}R_{23}\rangle_s. \tag{51}$$

For a V-type sample, Fig. 8 shows the steady-state fluorescence spectrum, where the left column corresponds to $N=10$ and the right column is for $N=100$, while the upper row displays the case $\mathcal{C}=0.5$ and the lower row shows the case $\mathcal{C}=4$. The solid lines correspond to a relative phase $\Delta\phi=\pi/2$, i.e., $X_V=\mathcal{C}$. The dashed lines are drawn for $X_V=1$ which is equivalent to $\Delta\phi=\pi(\Delta\phi=\cos^{-1}3/4)$ for $\mathcal{C}=0.5(\mathcal{C}=4)$. The main properties of the collective spectral lines are as follows. If $X_V=1$, then the widths of all lines are the same as for a single atom, while the peak intensities are proportional to the squared number of atoms, N^2. If $X_V<1$, then the spectral widths for all bands and the peak intensities for the lines at $\pm\tilde{\Omega}$ are proportional to the number of atoms N, while the peak intensities of the lines located at $\{\pm 2\tilde{\Omega},0\}$ are independent of N. For $X_V>1$ the spectral widths are a linear function of N for the spectral lines at $\pm\tilde{\Omega}$, while the intensities are independent of N for these lines. The spectral widths for the bands at $\{\pm 2\tilde{\Omega},0\}$ are the same as for a single atom, while the intensities scale as N^2.

Figure 9 depicts the corresponding results for a Λ-type sample. Here, the solid lines are drawn for $\Delta\phi=0$, i.e., $X_\Lambda\to\infty$. The dashed lines correspond to $X_\Lambda=1$ or $\Delta\phi=\pi(\Delta\phi=\cos^{-1}3/4)$ for $\mathcal{C}=0.5(\mathcal{C}=4)$. If $X_\Lambda=1$, then the peak intensities of all five spectral lines scale as N^2, while the spectral widths are the same as for a single atom. For $X_\Lambda<1$, the peak intensities of the spectral bands are independent of N, while their spectral widths are a linear function of N. If $X_\Lambda>1$, then the peak intensities and the spectral widths of the lines located at $\pm\tilde{\Omega}$ depend linearly on N. At frequencies $\{\pm 2\tilde{\Omega},0\}$, the peak intensities are proportional to the squared number of atoms and the widths are the same as for a single atom.

From the explicit expressions for the collective fluorescence spectra of both V- and Λ-type samples one can observe that due to the presence of the cross-damping terms the relative intensities of the spectral components emitted at frequencies $\{\omega_0\pm\tilde{\Omega}\}$ vanish for $\Delta\phi=2n\pi$ and $\tilde{\theta}=\pi/4$, while the intensities corresponding to the spectral components generated at $\{\omega_0,\omega_0\pm 2\tilde{\Omega}\}$ are always zero for $\Delta\phi=(2n+1)\pi$, $\{n\in 0,1,2,\ldots\}$. These properties are valid for any number of atoms in the sample.

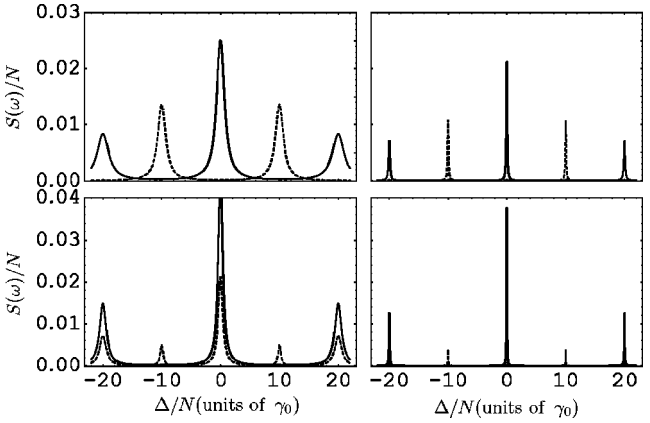

FIG. 9. The same as Fig. 8, but for the Λ sample, $\Delta\phi=0$ for the solid lines, $\Delta\phi=\pi(\Delta\phi=\cos^{-1}3/4)$ for the dashed lines, and $\mathcal{C}=0.5(\mathcal{C}=4)$.

Figure 10 shows the dependence of the steady-state collective intensities of the spectral lines located at $\pm\tilde{\Omega}$ (left column) and $\{0,\pm 2\tilde{\Omega}\}$ (right column) for the V- and Λ- type sample, respectively, as a function of the ratio $\mathcal{C}$.

From the main properties of the spectral lines discussed above, for a large V system one has $I^{(V)}_{\pm\tilde{\Omega}}=0$ only for $\mathcal{C}>1(X_V>1)$. For $\mathcal{C}<1(X_V<1)$, or for $\Delta\phi=\pi$, one finds $I^{(V)}_{0,\pm 2\tilde{\Omega}}=0$. If $\tilde{\theta}=\pi/4$ and $\Delta\phi=\pi$, then this intensity vanishes for any N since then $\Omega_+^2=0$.

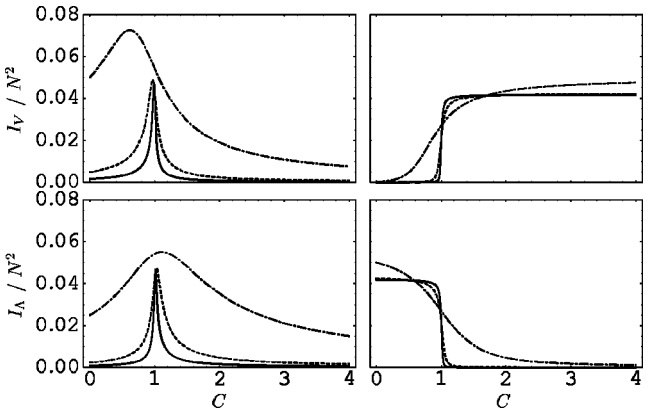

FIG. 10. The variance of the steady-state collective intensities of the spectral bands against the ratio $\mathcal{C}$. The upper row is for V-type systems, the lower for Λ-type samples. The left column corresponds to the sidebands located at $\omega_0\pm\tilde{\Omega}$ and the right one to the spectral lines emitted at $\{\omega_0,\omega_0\pm 2\tilde{\Omega}\}$. All figures are for $\Delta\phi=\pi/2$. The dash-dotted, dashed, and solid curves correspond to $N=10$, 100, and 300, respectively.

For a large Λ-type system both $I^{(\Lambda)}_{\pm\tilde{\Omega}}$ and $I^{(\Lambda)}_{0,\pm 2\tilde{\Omega}}$ are equal to zero for $\mathcal{C}>1 (X_\Lambda<1)$. Also, for $\tilde{\theta}=\pi/4$ and $\Delta\phi=\pi$, one has $\Omega_+^2=0$ and thus $I^{(\Lambda)}_{0,\pm 2\tilde{\Omega}}=0$ for any number of atoms.

The total steady-state intensity $I_{V(\Lambda)}$ of the collective fluorescence light emitted spontaneously on both transitions $|2\rangle\leftrightarrow|1\rangle$ and $|3\rangle\leftrightarrow|1\rangle$ may be evaluated from Eq. (41) to give

$$I_V=\frac{\Omega_-^2}{2\tilde{\Omega}^2}[N(\langle R\rangle_s+2)-\langle R^2\rangle_s-2\langle R\rangle_s]+\frac{\Omega_+^2}{4\tilde{\Omega}^2}\langle R_+\rangle_s,$$

$$I_\Lambda=\frac{\Omega_-^2}{2\tilde{\Omega}^2}[(N+1)\langle R\rangle_s-\langle R^2\rangle_s]+\frac{\Omega_+^2}{4\tilde{\Omega}^2}\langle R_+\rangle_s, \qquad (52)$$

with $\langle R_+\rangle_s=2[\langle R^2\rangle_s+2\langle R\rangle_s]/3$. First, we investigate the case $\eta=1$, $\tilde{\theta}=\pi/4$ with $\mathcal{C}=0.5$ or 4. Figures 3(c) and 3(d) show the collective steady-state fluorescence intensity per emitted atom I_V/N^2 for a V system. Minima occur around $\Delta\phi=\pi n$ for $n\in\{0,1,2,\ldots\}$. A comparison with Figs. 3(a) and 3(b) shows that the minima occurring for *even* $n(X_V=0)$ are due to the trapping of the population in the collective dressed state $|\Psi_1\rangle$, i.e., in the collective upper bare states $|2\rangle$ and $|3\rangle$. In Fig. 3(c), the fluorescence intensity also tends to zero for $N\gg 1$ at phase differences corresponding to *odd n*. However, the population is not trapped in $|\Psi_1\rangle$ at these phase differences, but distributes equally over the two other dressed states. Thus 0.5 of the atomic population is in the ground bare state $|1\rangle$, while 0.25 of the population is in each of the upper bare states $|2\rangle$ and $|3\rangle$. Because there is no inhibition of fluorescence for a single atom, these minima may be interpreted as arising from subradiant states: One-half of the population is in the excited state, and any emission from the excited state is absorbed by the other half of the population in the ground state. In Fig. 3(d), for smaller values of $\mathcal{C}$, the dark states at odd *n* do not occur, and even the local minima at the corresponding phase differences eventually disappear with sufficiently intense repumping for $\mathcal{C}<0.5$ (or $X_Y<1$). In this case the radiation intensity scales linearly with *N*, as it does for an ensemble of independent emitters.

In a large Λ sample ($N\gg 1$), the fluorescence may be suppressed for $\Delta\phi=\pi(2n+1)$ with $n\in\{0,1,2,\ldots\}$ if the decay dominates over the repumping as shown in Fig. 4(c). This inhibition is due to the trapping of the population in the collective dressed state $|\Psi_1\rangle$ as already found for even *n* in the V system, though here only for large *N*. For $\Delta\phi=2\pi n(X_\Lambda\to\infty)$, the collective steady-state intensity is maximal and proportional to the squared number of atoms $N^2[I_\Lambda=N(2+N)/3]$. Then, 0.5 of the population is in the upper bare state $|1\rangle$, and 0.25 of the population in each ground bare state $|2\rangle$ and $|3\rangle$. Thus this setting can be interpreted as a superradiant state. This superradiant state is analogous to the intense-field limit of collective resonance fluorescence from a system of two-level emitters [15], where the superradiant behavior is due to the quantum fluctuations of the vacuum. With increased pumping [see Fig. 4(d) with $\mathcal{C}=0.5$], no trapping can be observed and the maxima at $\Delta\phi=\pi(2n+1)$ eventually vanish as the intensity is proportional to *N* for $\mathcal{C}<0.5$ (or $X_\Lambda>1$). Here, for even *n*, the *N* dependence is quadratic while it is linear for odd *n*.

Figures (5) and (6) (second row) show the steady-state collective intensities emitted on both transitions $|2\rangle\leftrightarrow|1\rangle$ and $|3\rangle\leftrightarrow|1\rangle$ in V and Λ atoms, but with $\eta=0$ and 1, respectively. In Fig. 5, three cases for $\mathcal{C}$ can be distinguished. For $\mathcal{C}<1$ and large *N*, one finds $I_V=N$ and $I_\Lambda=N(N+5)/6$. Thus, for V atoms, only the spectral lines emitted at $\omega_0\pm\tilde{\Omega}$ contribute to the fluorescence intensity, while for the Λ radiators the contribution comes from all five spectral bands. If $\mathcal{C}=1$, then $I_V=I_\Lambda=N(N+3)/6$ and all five spectral lines contribute to the collective intensity for both system types. If $\mathcal{C}>1$, then $I_V=N(N+2)/6$, but $I_\Lambda=0$. Here, the spectral bands at frequencies ω_0, $\omega_0\pm 2\tilde{\Omega}$ contribute to the spectral intensity of the V-type atoms. Thus for $\eta=0$ and $N\gg 1$, the suppression of the collective fluorescence intensity may only be observed for the Λ system. For the phase-dependent scheme with $\Delta\phi=\pi$ (see Fig. 6), inhibition of the collective resonance fluorescence occurs for large V-type samples for $X_V>1$ and for large Λ-type samples when $X_\Lambda<1$ (or $\mathcal{C}>0.5$). Thus the emission properties of the V-type atomic sample depend strongly on the relative phase between the applied external coherent fields. In particular, the inhibition of the total fluorescence light emitted by such a V sample occurs only for the phase-dependent scheme.

B. Magnetic and thermal influences on the collective spectral features

If the emitters are surrounded by a thermal bath rather than the usual vacuum, the resonance fluorescence spectrum has the same form as Eq. (41), but with modified parameters. For the nondegenerate atomic samples, with $\theta\neq 0$, the collective spectral widths of the spectral components emitted at frequencies $\{\omega_0\pm\Omega,\omega_0\pm 2\Omega,\omega_0\}$ are given by

$$\Gamma_{V(\Lambda)}=\gamma_{V(\Lambda)}\mp\gamma_0\sin^2\theta[N-2\langle R_{11}\rangle_s],$$

$$\tilde{\Gamma}_{V(\Lambda)}=\tilde{\gamma}_{V(\Lambda)}\pm 2\gamma_0\sin^2\theta\langle R_{11}\rangle_s,$$

$$\bar{\Gamma}_{V(\Lambda)}=\bar{\gamma}_{V(\Lambda)}\pm 2\gamma_0\sin^2\theta\langle R_{11}\rangle_s, \qquad (53)$$

where the corresponding single-atom spectral widths are given by

$$\gamma_V=\gamma_0(1+\bar{n}+2\bar{n}\sin^2\theta), \qquad (54)$$

$$\tilde{\gamma}_V=\gamma_0(1+\bar{n})(2+\cos^2\theta), \qquad (55)$$

$$\bar{\gamma}_V=2\gamma_0(1+\bar{n}), \qquad (56)$$

and

$$\gamma_\Lambda=\gamma_0(1+\bar{n})+\gamma_0(1+2\bar{n})\sin^2\theta, \qquad (57)$$

$$\tilde{\gamma}_\Lambda=2\gamma_0\bar{n}\sin^2\theta+3\gamma_0(1+\bar{n})\cos^2\theta, \qquad (58)$$

$$\bar{\gamma}_\Lambda=2\gamma_0(\bar{n}+\cos^2\theta). \qquad (59)$$

The peak intensities of the spectral lines are given by

$$I^{(V)}_{\pm\Omega} = \sin^2\theta\langle R_{21}R_{12}\rangle_s, \tag{60}$$

$$I^{(V)}_{\pm 2\Omega,0} = \frac{1}{2}\cos^2\theta\langle R_{23}R_{32}\rangle_s, \tag{61}$$

$$I^{(\Lambda)}_{\pm\Omega} = \sin^2\theta\langle R_{12}R_{21}\rangle_s, \tag{62}$$

$$I^{(\Lambda)}_{\pm 2\Omega,0} = \frac{1}{2}\cos^2\theta\langle R_{32}R_{23}\rangle_s. \tag{63}$$

For the degenerate atomic systems, with $\tilde{\theta}\neq\pi/4$, the corresponding results are

$$\Gamma_{V(\Lambda)} = \gamma_{V(\Lambda)} \pm \frac{\gamma_0}{2}[1-\sin 2\tilde{\theta}][N-2\langle R_{11}\rangle_s],$$

$$\tilde{\Gamma}_{V(\Lambda)} = \tilde{\gamma}_{V(\Lambda)} \mp \gamma_0[1-\sin 2\tilde{\theta}]\langle R_{11}\rangle_s,$$

$$\overline{\Gamma}_{V(\Lambda)} = \overline{\gamma}_{V(\Lambda)} \mp \gamma_0[1-\sin 2\tilde{\theta}]\langle R_{11}\rangle_s, \tag{64}$$

with

$$\gamma_V = \gamma_0(1+2\overline{n}) + \frac{\gamma_0}{2}(1+\overline{n})(1-\sin 2\tilde{\theta}), \tag{65}$$

$$\tilde{\gamma}_V = \gamma_0\overline{n}(1-\sin 2\tilde{\theta}) + \frac{3}{2}\gamma_0(1+2\overline{n})(1+\sin 2\tilde{\theta}), \tag{66}$$

$$\overline{\gamma}_V = \gamma_0\overline{n}(1-\sin 2\tilde{\theta}) + \gamma_0(1+2\overline{n})(1+\sin 2\tilde{\theta}), \tag{67}$$

$$\gamma_\Lambda = \gamma_0(1+2\overline{n}) + \frac{\gamma_0}{2}\overline{n}(1-\sin 2\tilde{\theta}), \tag{68}$$

$$\tilde{\gamma}_\Lambda = \gamma_0(1+\overline{n})(1-\sin 2\tilde{\theta}) + \frac{3}{2}\gamma_0(1+2\overline{n})(1+\sin 2\tilde{\theta}), \tag{69}$$

$$\overline{\gamma}_\Lambda = \gamma_0(1+\overline{n})(1-\sin 2\tilde{\theta}) + \gamma_0(1+2\overline{n})(1+\sin 2\tilde{\theta}), \tag{70}$$

and

$$I^{(V)}_{\pm\tilde{\Omega}} = \frac{1}{2}[1-\sin 2\tilde{\theta}]\langle R_{12}R_{21}\rangle_s, \tag{71}$$

$$I^{(V)}_{\pm 2\tilde{\Omega},0} = \frac{1}{4}[1+\sin 2\tilde{\theta}]\langle R_{32}R_{23}\rangle_s, \tag{72}$$

$$I^{(\Lambda)}_{\pm\tilde{\Omega}} = \frac{1}{2}[1-\sin 2\tilde{\theta}]\langle R_{21}R_{12}\rangle_s, \tag{73}$$

$$I^{(\Lambda)}_{\pm 2\tilde{\Omega},0} = \frac{1}{4}[1+\sin 2\tilde{\theta}]\langle R_{23}R_{32}\rangle_s. \tag{74}$$

Note that the exact strong-field single-atom expressions for the emission spectra can be obtained from Eq. (41) by dropping the collective contributions in the spectral widths which are then broadened only by the thermal reservoir.

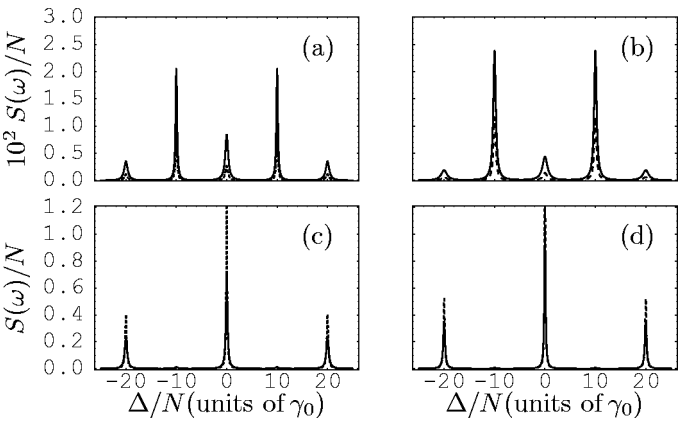

FIG. 11. The steady-state fluorescence spectrum as a function of the detuning Δ. The left plots belong to a V system, the right ones to a Λ sample. (a), (d) correspond to $\Omega_2=\Omega_3$ and $\omega_{23}\neq 0$, while (b), (c) correspond to $\omega_{23}=0$ and $\Omega_2\neq\Omega_3$ (independent of the precise values). Here, $N=25$; solid line, $\overline{n}=1$; dashed line, $\overline{n}=0.4$; $\sin^2\theta=\sin^2\tilde{\theta}=0.1$; and $\Omega=\tilde{\Omega}=10N\gamma_0$.

For a large V(Λ) sample ($N\gg 1$) with nondegenerate upper bare states (degenerate lower bare states) and bath temperatures with $X_V<1(X_\Lambda<1)$ the collective intensities of all spectral lines are zero, i.e., $I^{(V)}_{\pm\Omega}=I^{(V)}_{\pm 2\Omega,0}=0(I^{(\Lambda)}_{\pm\tilde{\Omega}}=I^{(\Lambda)}_{\pm 2\tilde{\Omega},0}=0)$ [see Figs. 11(a), 11(b), 12(a), and 12(b)]. The inhibition of the collective resonance fluorescence in this case is due to trapping of all population in the dressed state $|\Psi_{11}\rangle$ (see Fig. 7), i.e., $\langle R_{11}\rangle_s\to N$ while both $\langle R\rangle_s$ and $\langle R^2\rangle_s$ tend to zero. For a large V(Λ) sample with degenerate upper bare states (nondegenerate lower bare states) and low temperatures the peak intensities of the spectral bands generated at $\omega_0\pm\tilde{\Omega}(\omega_0\pm\Omega)$ vanish identically, i.e., $I^{(V)}_{\pm\tilde{\Omega}}=0(I^{(\Lambda)}_{\pm\Omega}=0)$ [see Figs. 11(a), 11(b), 12(a), and 12(b)]. Then the peak intensities $I^{(V)}_{\pm 2\tilde{\Omega},0}(I^{(\Lambda)}_{\pm 2\Omega,0})$

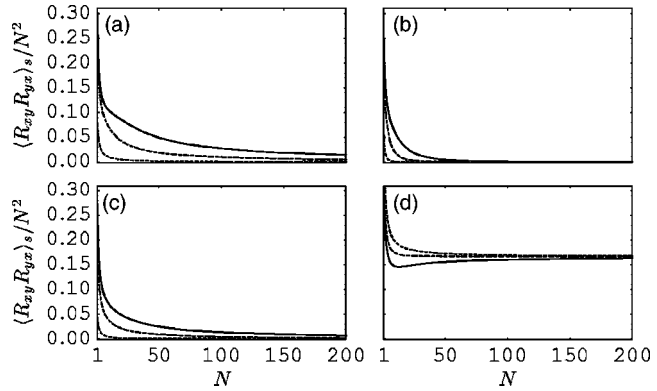

FIG. 12. The steady-state dependence of the spectral peak intensities as a function of the number of atoms N, generated at (a) $\omega_0\pm\Omega(\omega_0\pm\tilde{\Omega})$ with subindices $x=2$, $y=1$; (b) $\omega_0\pm 2\Omega$, $\omega_0(\omega_0\pm 2\overline{\Omega},\omega_0)$ with $x=2$, $y=3$; (c) $\omega_0\pm\tilde{\Omega}(\omega_0\pm\Omega)$ with $x=1$, $y=2$; (d) $\omega_0\pm 2\tilde{\Omega}$, $\omega_0(\omega_0\pm 2\Omega,\omega_0)$ with $x=3$, $y=2$, corresponding to V- (Λ-)type samples, respectively. Further the dashed, dash-dotted, and solid lines are plotted for $\overline{n}=0.1$, 1, and 3, respectively.

emitted at $\omega_0 \pm 2\widetilde{\Omega}, \omega_0 (\omega_0 \pm 2\Omega, \omega_0)$ are proportional to the squared number of atoms [see Figs. 11(a), 11(b), 12(a), and 12(b)]. The widths of all three spectral lines are the same as for a single atom, because for $\bar{n} \ll 1$ one has $X_V, X_\Lambda \gg 1$ and therefore $\langle R_{11} \rangle_s \to 0$, $\langle R \rangle_s \to N$ but $\langle R^2 \rangle_s \to N^2$.

For a degenerate V-type system (nondegenerate Λ-type system), the spectral peak intensities generated at $\{\omega_0 \pm 2\widetilde{\Omega}, \omega_0\} (\omega_0 \pm 2\Omega, \omega_0)$ exhibit a minimum that is more pronounced with increasing $\bar{n}$ [see Fig. 12(d)]. To explain its origin we represent the intensities of these lines via the dressed-state atomic correlators

$$I^{(V)}_{\pm 2\widetilde{\Omega},0} \propto I^{(\Lambda)}_{\pm 2\Omega,0} \propto \langle R_{23} R_{32} \rangle_s = \langle R_{32} R_{23} \rangle_s = \langle R \rangle_s / 3 + \langle R^2 \rangle_s / 6 \tag{75}$$

with $X_V(\omega_{23}=0) = X_\Lambda(\omega_{23} \neq 0) = 1 + 1/\bar{n}$. For a weak thermal bath, i.e., $\bar{n} \ll 1$, one has $X \gg 1$ and thus $I^{(V)}_{\pm 2\widetilde{\Omega},0} (I^{(\Lambda)}_{\pm 2\Omega,0}) = N/3 + N^2/6$, while for an intense thermal bath with $\bar{n} \gg 1$, one has $X \approx 1$ and $I^{(V)}_{\pm 2\widetilde{\Omega},0} (I^{(\Lambda)}_{\pm 2\Omega,0}) = N/4 + N^2/12$. Thus in the second case (with $X \approx 1$) the collective emitted EMF is weaker. Note that Figs. 11(d) and 12(d) are plotted for intermediate values, i.e., for values of X between $X \approx 1$ and $X \gg 1$. Figure 7 (lower line) further shows the dependence of the total fluorescence intensity on both the thermal photon number $\bar{n}$ and the splitting frequency between the closely spaced bare states. Just as for the populations, changing the system from degenerate to nondegenerate or vice versa corresponds to jumps between the branches in Fig. 7, demonstrating the large changes in the sample properties induced by small changes in the external parameters.

Thus, we have shown various ways to modify the collective resonance fluorescence in driven three-level samples. By suitably choosing the configuration of the external parameters, it is possible to suppress the total fluorescence intensity or the intensity of some of the spectral peaks of the fluorescence spectrum. As with the steady-state population distribution, this again is an advantage over corresponding schemes involving ensembles of two-level atoms [15], where for example an inhibition of the fluorescence is difficult to achieve.

VI. THE COLLECTIVE ABSORPTION SPECTRUM

Next we discuss the absorption properties of the atomic samples. We suppose that an additional weak probe field of frequency ν drives both transitions $|2\rangle \leftrightarrow |1\rangle$ and $|3\rangle \leftrightarrow |1\rangle$ of the V- (Λ)-type atomic system. According to the linear-response theory, the absorption spectrum of the weak field can be calculated by the following relation [15]:

$$W_a(\nu) \propto \mathrm{Re}\left\{ \lim_{t \to \infty} \int_0^t d\tau\, e^{i(\omega_0 - \nu)\tau} W_a(t+\tau, t) \right\} \tag{76}$$

where $W_a(t+\tau, t) = \langle [S^-(t+\tau), S^+(t)] \rangle$ with

$$S^-_V = d_2 S_{12} e^{i\phi_2} + d_3 S_{13} e^{i\phi_3} \tag{77}$$

for the V system,

$$S^-_\Lambda = d_2 S_{21} e^{i\phi_2} + d_3 S_{31} e^{i\phi_3} \tag{78}$$

for the Λ sample, and $S^+ = [S^-]^\dagger$.

A. Phase manipulation of the absorption properties

In the following we investigate the possibility of controlling the absorption properties of the degenerate three-level samples using the relative phase between the applied strong coherent fields. Introducing Eq. (11) in Eq. (76), and making use of the secular approximation, for a V sample we obtain the following expression for the absorption spectrum:

$$W^{(V)}_a(\nu) = \mathrm{Re} \int_0^\infty d\tau\, e^{i(\omega_0 - \nu)\tau} \Bigg[\frac{\Omega_-^2}{2\Omega^2} \{ \langle [R_{21}(\tau), R_{12}] \rangle + \langle [R_{31}(\tau), R_{13}] \rangle \} + \frac{\Omega_+^2}{4\Omega^2} \{ \langle [R_{23}(\tau), R_{32}] \rangle + \langle [R_z(\tau), R_z] \rangle + \langle [R_{32}(\tau), R_{23}] \rangle \} \Bigg]. \tag{79}$$

By inserting Eq. (33) in Eq. (79), one can arrive at the following expression for the absorption spectrum of a weak probe field:

$$W^{(i)}_a(\nu) = \alpha_i \left[\frac{\Gamma_i}{\Gamma_i^2 + (\Delta_p + \widetilde{\Omega})^2} + \frac{\Gamma_i}{\Gamma_i^2 + (\Delta_p - \widetilde{\Omega})^2} \right] \tag{80}$$

where $i \in \{V, \Lambda\}$, $\Delta_p = \omega_0 - \nu$, and $\alpha_{V(\Lambda)} = (\Omega_-^2 / 2\widetilde{\Omega}^2) \times [\pm \langle R \rangle_s / 2 \mp \langle R_{11} \rangle_s]$. Because the steady-state populations in the dressed states $|\Psi_2\rangle$ and $|\Psi_3\rangle$ are equal, the last term in Eq. (79), which is proportional to Ω_+^2, does not contribute. From Eq. (80) it can be seen that for the particular case of identical Rabi frequencies, i.e., $\widetilde{\theta} = \pi/4$ and $\Delta\phi = 2n\pi$ ($n = 0, 1, 2, \ldots$), the absorption of both V and Λ samples vanishes. The exact strong-field single-atom absorption spectra can be obtained from Eq. (80) by dropping the collective contributions in the absorption linewidths. Figures 13 and 14 depict the steady-state dependence of the collective absorption amplitude of an additional weak coherent field that drives one or both atomic transitions in a V or Λ sample, respectively, versus the relative phase between the strong external lasers. The interpretation of these results is straightforward if one considers Figs. 3 and 4. For a V-type sample with $\mathcal{C} = 0.5$, $\widetilde{\theta} = \pi/4$, and $\Delta\phi = 2\pi n$ almost all of the population will be in the collective dressed state $|\Psi_1\rangle$ for even n. This means that all the atoms are equally distributed among the degenerate upper bare states and, thus, an additional weak coherent field probing one of the transitions will be amplified. For odd n and $\mathcal{C} = 0.5$, $\widetilde{\theta} = \pi/4$ the bare atomic states are approximately identically populated so that the absorption will be zero (see top left figure in Fig. 13). A similar explanation also holds if the additional probing field drives both transitions. For example, for $\mathcal{C} = 2$, $\widetilde{\theta} = \pi/4$, and odd n the probing field is absorbed as in this case there are more atoms in the ground state than in each of the upper states. In case of even n the probing field remains unmodified when it is coupled to both transitions, as $\Omega_-^2 = 0$. The degenerate Λ

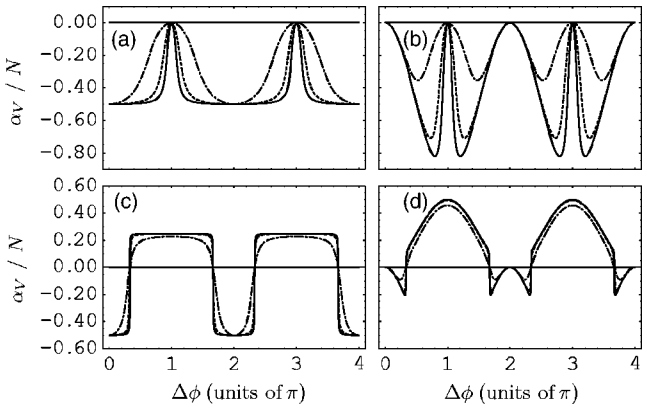

FIG. 13. The steady-state dependence of the collective absorption amplitude of an additional weak coherent field [which drives the transitions $|1\rangle \leftrightarrow |2\rangle$ (left column) or simultaneously both transitions (right column) in a degenerate V sample] versus the relative phase between the strong applied lasers. The upper line stands for $\mathcal{C}=0.5$, while the lower one represents $\mathcal{C}=2$ and $\tilde{\theta}=\pi/4$. Dash-dotted, dashed, and solid curves are plotted for $N=10$, 100, and 300, respectively.

sample (see Fig. 14) may be interpreted along the same lines. Thus, by adjusting external parameters such as the phase $\Delta\phi$ we can conveniently manipulate the absorption properties of a degenerate three-level V or Λ atomic sample.

B. Magnetic and thermal influences on the absorption processes

In this section we discuss the influences of a thermal bath on the absorption properties of our three-level samples. Introducing Eqs. (11) and (20) in Eq. (76) and utilizing the same procedure as we did for the collective resonance fluorescence spectra one can show that the expression for the absorption spectrum, in this case, has the same form as Eq. (80), but with

$$\alpha_{V(\Lambda)} = \sin^2\theta[\pm\langle R_{11}\rangle_s \mp \langle R\rangle_s/2] \tag{81}$$

for the nondegenerate atoms, and

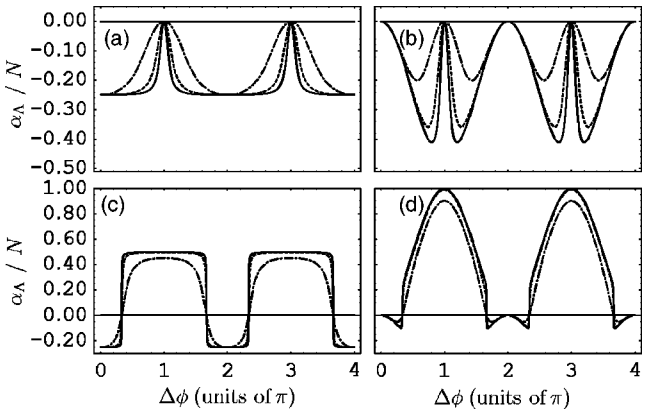

FIG. 14. The same as Fig. 13, but for the Λ sample.

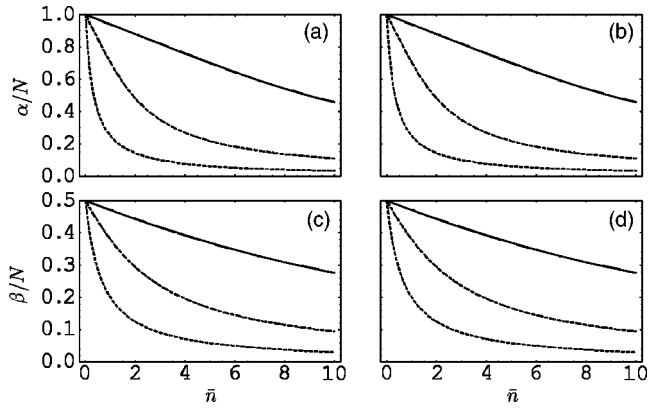

FIG. 15. The dependence of the steady-state absorption peak amplitudes $\alpha=\langle R_{11}\rangle_s-\langle R\rangle_s/2$ and $\beta=\langle R\rangle_s/2-\langle R_{11}\rangle_s$ versus the mean thermal photon number $\bar{n}$. The left plots belong to the V system, and the right ones to the Λ sample. (a), (d) correspond to the nondegenerate schemes, and (b), (c) to the degenerate ones. Here, the dashed, dash-dotted, and solid curves are plotted for $N=1$, 10, and 50, respectively.

$$\alpha_{V(\Lambda)} = \frac{\Omega_-^2}{2\tilde{\Omega}^2}[\pm\langle R\rangle_s/2 \mp \langle R_{11}\rangle_s] \tag{82}$$

for degenerate atoms with $\theta \neq 0$ and $\tilde{\theta} \neq \pi/4$, respectively. Note that the width $\Gamma_V(\Gamma_\Lambda)$ is different for nondegenerate and degenerate schemes (see the corresponding expression for the emission spectra). From the absorption amplitudes α_i one may see that the absorption characteristics can be manipulated by the environmental temperature. In particular, for an intense thermal bath with $\bar{n} \gg 1$, the absorption coefficients of both V and Λ samples vanish because the dressed states are equally populated in this case. However, these results are obtained in the secular approximation, that is, the generalized Rabi frequency must be larger than any other decay rates in the system. In other words, on heating the bath, one should also increase the Rabi frequency. This suggests that a small atomic sample is preferable in order to obtain zero absorption or, in the opposite case, very intense external coherent sources have to be used (see Fig. 15).

VII. SUMMARY

Concluding, we have investigated analytically the steady-state behavior of a collection of strongly driven V- or Λ-type atoms depending on external parameters such as the relative phase between two applied strong driving laser fields, the ratio of spontaneous decay and incoherent pumping rates, the splitting frequency between closely spaced atomic states, or a surrounding thermal bath. It was shown that the interplay of decay and pumping processes in degenerate three-level atomic samples allows for a rapid coherent phase control of collective population dynamics along with the feasibility of transferring the atoms conveniently into sub- or superradiant ensembles. It should be noted that the discussed phase control depends crucially on the presence of incoherent pumping as a counterpart to the phase-dependent dressed decay rates.

We have further discussed the case where the three-level emitters are surrounded by a thermal bath. Increasing the temperature of the environment generally decreases the maximum population that can be transferred into or out of the discussed dressed state. This effect, however, is less pronounced in larger samples. In this setup, the steady state of the system is also strongly dependent on the frequency difference between the two closely spaced upper (lower) levels in the V(Λ) configuration. Thus by slightly varying this splitting via an external magnetic field and by changing the intensities of the driving fields, the direction of the dressed spontaneous decay can be reversed which accounts for large changes in the steady-state population distribution.

Together with the steady state of the populations, also the collective steady-state radiation and absorption properties are changeable over wide ranges by varying these control parameters. We have found configurations where the total fluorescence intensity is suppressed, or where some of the emission peaks in the spectrum vanish, thus changing the spectral composition of the emitted light. All of these features can be explained in terms of the discussed steady-state solutions for the populations, allowing for a clear separation of effects which are present only in collective systems. The same holds for the absorption properties, where both positive and negative gain for the probe beam can be achieved by varying the above control parameters.

Finally, we have discussed the time evolution of the dressed populations to show that the presented schemes feature a rapid transfer into the respective steady states, thus allowing for possible applications such as fast optical switching devices.

ACKNOWLEDGMENTS

Financial support is acknowledged from the Alexander-von-Humboldt Foundation for M.M., by the German Science Foundation for J.E. and C.H.K., and by the German National Academic Foundation for J.E.

[1] M. O. Scully and M. S. Zubairy, *Quantum Optics* (Cambridge University Press, Cambridge, U.K., 1997).
[2] R. H. Dicke, Phys. Rev. **93**, 99 (1954).
[3] R. H. Lehmberg, Phys. Rev. A **2**, 883 (1970); **2**, 889 (1970).
[4] L. Allen and J. H. Eberly, *Optical Resonance and Two-Level Atoms* (Wiley, New York, 1975).
[5] M. Gross and S. Haroche, Phys. Rep. **93**, 301 (1982).
[6] A. V. Andreev, V. I. Emel'yanov, and Yu. A. Il'inskii, *Cooperative Effects in Optics: Superfluorescence and Phase Transitions* (IOP Publishing, London, 1993).
[7] N. Skribanowitz, I. P. Herman, J. C. MacGillivray, and M. S. Feld, Phys. Rev. Lett. **30**, 309 (1973); C. Greiner, B. Boggs, and T. W. Mossberg, *ibid.* **85**, 3793 (2000).
[8] D. Pavolini, A. Crubellier, P. Pillet, L. Cabaret, and S. Liberman, Phys. Rev. Lett. **54**, 1917 (1985).
[9] H. W. Chan, A. T. Black and V. Vuletic, Phys. Rev. Lett. **90**, 063003 (2003).
[10] S. John and T. Quang, Phys. Rev. Lett. **74**, 3419 (1995).
[11] N. A. Enaki and M. A. Macovei, Zh. Eksp. Teor. Fiz. **115**, 1153 (1999) [JETP **88**, 633 (1999)].
[12] C. H. Keitel, M. O. Scully, and G. Süssmann, Phys. Rev. A **45**, 3242 (1992).
[13] V. Kozlov, O. Kocharovskaya, Y. Rostovtsev, and M. Scully, Phys. Rev. A **60**, 1598 (1999).
[14] F. Haake, M. I. Kolobov, C. Fabre, E. Giacobino, and S. Reynaud, Phys. Rev. Lett. **71**, 995 (1993); F. Haake, M. I. Kolobov, C. Seeger, C. Fabre, E. Giacobino, and S. Reynaud, Phys. Rev. A **54**, 1625 (1996).
[15] R. R. Puri, *Mathematical Methods of Quantum Optics* (Springer, Berlin 2001), especially Chap. 12 and references therein.
[16] M. Lewenstein and J. Javanainen, Phys. Rev. Lett. **59**, 1289 (1987); M. S. Kim, F. A. M. de Oliveira, and P. L. Knight, Opt. Commun. **70**, 473 (1989); P. I. Bardetski, and M. A. Macovei, Phys. Scr. **67**, 306 (2003).
[17] N. N. Bogolubov, Jr., T. Quang, and A. S. Shumovsky, Phys. Lett. **112A**, 323 (1985); A. S. Shumovsky, R. Tanas, and T. Quang, Opt. Commun. **64**, 45 (1987); S. Ya. Kilin, Zh. Eksp. Teor. Fiz. **82**, 63 (1982) [Sov. Phys. JETP **55**, 38 (1982)].
[18] M. Macovei and C. H. Keitel, Phys. Rev. Lett. **91**, 123601 (2003).
[19] M. Macovei, J. Evers, and C. H. Keitel, Phys. Rev. Lett. **91**, 233601 (2003).
[20] M. Macovei, J. Evers, and C. H. Keitel, Europhys. Lett. **68**, 391 (2004).
[21] M. A. Macovei and J. Evers, Opt. Commun. **240**, 379 (2004).
[22] M. D. Lukin, M. Fleischhauer, R. Cote, L. M. Duan, D. Jaksch, J. I. Cirac, and P. Zoller, Phys. Rev. Lett. **87**, 037901 (2001).
[23] C. P. Sun, S. Yi, and L. You, Phys. Rev. A **67**, 063815 (2003).
[24] L.-M. Duan, J. I. Cirac, P. Zoller, and E. S. Polzik, Phys. Rev. Lett. **85**, 5643 (2000); B. Julsgaard, A. Kozhekin, and E. S. Polzik, Nature (London) **413**, 400 (2001); L.-M. Duan, Phys. Rev. Lett. **88**, 170402 (2002); A. Messikh, Z. Ficek, and M. R. B. Wahiddin, J. Opt. B: Quantum Semiclassical Opt. **5**, L1 (2003).
[25] P. Domokos and H. Ritsch, Phys. Rev. Lett. **89**, 253003 (2002).
[26] M. A. G. Martinez, P. R. Herczfeld, C. Samuels, L. M. Narducci, and C. H. Keitel, Phys. Rev. A **55**, 4483 (1997).
[27] E. Paspalakis and P. L. Knight, Phys. Rev. Lett. **81**, 293 (1998).
[28] J.-H. Wu and J.-Y. Gao, Phys. Rev. A **65**, 063807 (2002).
[29] T. Quang, M. Woldeyohannes, S. John, and G. S. Agarwal, Phys. Rev. Lett. **79**, 5238 (1997).
[30] C. Chen, Y-Y. Yin, and D. S. Elliott, Phys. Rev. Lett. **64**, 507 (1990); C. Chen, and D. S. Elliott, *ibid.* **65**, 1737 (1990); L. Zhu, K. Suto, J. A. Fiss, R. Wada, T. Seideman, and R. J. Gordon, *ibid.* **79**, 4108 (1997).
[31] Z. Ficek and S. Swain, J. Mod. Opt. **49**, 3 (2002); J. Evers and C. H. Keitel, Phys. Rev. Lett. **89**, 163601 (2002).
[32] G. S. Agarwal and S. Menon, Phys. Rev. A **63**, 023818 (2001);

P. Zhou, S. Swain, and L. You, *ibid.* **63**, 033818 (2001).
[33] P. Meystre and M. Sargent, *Elements of Quantum Optics* (Springer, Berlin, 1990).
[34] N. N. Bogolyubov and N. N. Bogolyubov, Jr., Fiz. Elem. Chastits At. Yadra **11**, 245 (1980) [Sov. J. Part. Nucl. **11**, 93 (1980)].
[35] G. S. Agarwal, *Quantum Statistical Theories of Spontaneous Emission and Their Relation to Other Approaches* (Springer, Berlin, 1974).
[36] A. K. Patnaik and G. S. Agarwal, Phys. Rev. A **59**, 3015 (1999); P. Zhou and S. Swain, Opt. Commun. **179**, 267 (2000).
[37] S. John and T. Quang, Phys. Rev. Lett. **78**, 1888 (1997).
[38] T. Quang and V. Buzek, J. Opt. Soc. Am. B **7**, 1487 (1990).
[39] S. Menon and G. S. Agarwal, Phys. Rev. A **57**, 4014 (1998).
[40] D. F. Walls and G. J. Milburn, *Quantum Optics* (Springer-Verlag, Berlin, 1994).